Prokaryotic Organelles: Bacterial Microcompartments in *E. coli* and *Salmonella*

Katie L. Stewart[1], **Andrew M. Stewart**[1], **Thomas A. Bobik**[1,*]

[1]The Roy J. Carver Department of Biochemistry, Biophysics and Molecular Biology, Iowa State University, Ames, IA, USA 50011

Abstract

Bacterial microcompartments (MCPs) are proteinaceous organelles consisting of a metabolic pathway encapsulated within a selectively permeable protein shell. Hundreds of species of bacteria produce MCPs of at least nine different types and MCP metabolism is associated with enteric pathogenesis, cancer, and heart disease. This review focuses chiefly on the four types of catabolic MCPs (metabolosomes) found in *E. coli* and *Salmonella:* the propanediol utilization (*pdu*), ethanolamine utilization (*eut*) choline utilization (*cut*), and glycyl radical propanediol (*grp*) MCPs. Although the great majority of work done on catabolic MCPs has been carried out with *Salmonella* and *E. coli*, research outside the group is mentioned where necessary for a comprehensive understanding. Salient characteristics found across MCPs are discussed, including enzymatic reactions and shell composition, with particular attention paid to key differences between classes of MCPs. We also highlight relevant research on the dynamic processes of MCP assembly, protein targeting and the mechanisms that underlie selective permeability. Lastly, we discuss emerging biotechnology applications based on MCP principles, and point out challenges, unanswered questions, and future directions.

General features of bacterial microcompartments (MCPs)

One often-cited mark of sophistication for eukaryotic cells is the ability to compartmentalize metabolic reactions. It is increasingly becoming appreciated, however, that prokaryotic cells also have the means to sequester cellular processes by the use of bacterial microcompartments (MCPs) [1–3]. MCPs range in size from 100 to 400 nm in diameter and consist of a selectively permeable protein shell surrounding enzymes for a multistep metabolic pathway. The pathways encapsulated within MCPs have volatile or toxic intermediates, and the primary functions of MCPs are to prevent cellular toxicity, reduce carbon loss, concentrate reaction machinery, and increase process efficiency. The genes required for MCP formation are typically contained within large contiguous gene clusters (Figure 1) that encode related elements and are frequently spread by horizontal gene transfer [3–8]. All known MCPs include shells that are built from a conserved set of shell proteins [9] and many catabolic MCPs encapsulate pathways involving radical enzymes that produce aldehyde intermediates [1, 5–7, 10]. MCPs are produced by hundreds of species of bacteria

*To whom correspondence should be addressed: Thomas A. Bobik, Iowa State University, Tel: (515) 294-8247, bobik@iastate.edu.

encompassing at least 23 phyla and have diverse physiological functions [4–8]. The metabolism of MCPs provides a selective advantage to pathogens in host environments and impacts the ecology of the human gut [1, 11–13]. Developments in characterizing the assembly and function of several classes of MCPs have revealed the complex nature of these particles and have motivated varied bioengineering applications [14–17]. However, there are still a number of unanswered questions surrounding MCPs that promise the discovery of unusual biochemistry and will likely spur further biotechnology advances.

Diverse bacterial MCPs

Carboxysomes were the first bacterial MCP identified [18]. Initially these compartments were observed within cyanobacteria by electron microscopy (EM) and thought to be viruses. However, later work showed that carboxysomes consisted of a protein shell filled with Rubisco and that their function was to enhance CO_2 fixation as part of a CO_2-concentrating mechanism [19–22]. Over 20 years later, an operon required for 1,2-propanediol utilization (*pdu*) by *S. enterica* Serovar Typhimurium (referred to here as *S. enterica*) was found to contain multiple homologs of carboxysome shell genes [22]. Further study showed that the *pdu* operon encoded a 100–150 nm polyhedral body (a new type of MCP) involved in 1,2-propanediol degradation [22]. Shortly after, searches of bacterial genomes for shell gene homologs began to identify diverse MCP operons which we now know are present in ~20% of bacterial species [4–8]. Further work found that catabolic MCPs (also referred to as metabolosomes) support bacterial growth on a variety of substrates including 1,2-propanediol, ethanolamine, choline, glycerol, rhamnose, fucose, fucoidan, aminoacetone and perhaps other metabolites [22–27].

This review focuses on metabolosomes found in *E. coli* and *Salmonella*. These include the propanediol utilization (*pdu*), ethanolamine utilization (*eut*), choline utilization (*cut*), and glycyl radical propanediol (*grp*) MCPs. Each of these metabolosomes support growth by breaking down substrates to alcohols and acids via acetaldehyde or propionaldehyde intermediates (Figure 2). The Pdu and Eut MCPs are the best studied metabolosomes and much of this research has been conducted in *Salmonella* and *E. coli* [10]. Both these MCPs use pathways that are dependent on coenzyme B_{12} (adenosylcobalamin), referred to here as Ado-B_{12}. The Cut and Grp MCPs employ glycyl radical enzymes and are B_{12}-independent [28–30]. They are part of the widespread group of MCPs known as glycyl radical microcompartments (GRMs) which are absent from *Salmonella*, but narrowly distributed among *E. coli*. These MCPs tend to be found in pathogenic strains where investigations aimed at dissecting their structure, function, mechanisms and unique features have recently begun [29, 30].

Function of the MCP Shell

The defining feature of MCPs is the presence of a selectively permeable, polyhedral protein shell. The shell itself plays three important functional roles: (1) protecting the cell from toxic intermediates generated by MCP enzymes, (2) sequestering volatile reaction intermediates, and (3) concentrating substrates together with reaction machinery. Both genetic and bioinformatic analyses support the idea that metabolosome shells protect cells from toxic aldehydes during substrate degradation [31]. Mutants unable to form the shell of the Pdu

MCP accumulate propionaldehyde to toxic levels and incur DNA damage. Furthermore, *polA* (DNA repair polymerase) and *gsh* (glutathione biosynthesis) mutants are impaired for growth on 1,2-propanediol or ethanolamine, supporting aldehyde toxicity [32]. In addition, under stringent conditions, *S. enterica* mutants unable to form the shell of the Eut MCP are incapable of growth due to acetaldehyde loss to the environment [33]. Other experiments on ethanolamine degradation showed that overexpression of Eut catabolic enzymes in the absence of the Eut MCP supported wild-type growth rates, indicating that another function of the MCP may be to concentrate reaction-associated enzymes [34]. Computational models of the Pdu MCP predict that the presence of the shell enhances pathway flux [35], similar to the role played by the carboxysome shell in increasing Rubisco activity [19]. Although specific functions have not been extensively tested in glycyl radical microcompartments, a conserved function seems reasonable. Thus, studies support the model that bacterial MCPs enhance metabolic pathways by sequestering toxic or volatile intermediates and by concentrating enzymes together with their substrates.

Role of MCPs in pathogenesis and human health

The metabolism of specific carbon substrates by MCPs confers a selective advantage to pathogenic bacteria in host environments and influences the ecology of the human gut in a manner that affects human health. Expression of the *eut* operon in *Salmonella* and *E. coli* is linked to virulence, including toxin production and increased transmission to new hosts [11, 36, 37], and is associated with UTIs and Crohns disease [38, 39]. Similarly, expression of the cobalamin (*cob*, B$_{12}$) biosynthesis-propanediol utilization *(cob-pdu)* gene cluster in *S. enterica* is necessary for replication within macrophages [40] and required for colonization of the gut lumen of host organisms [41]. Moreover, as a consequence of inflammation induced by *S. enterica* infection, chemical processes in the gut produce the unusual electron acceptor tetrathionate from thiosulfate which supports anaerobic respiration of ethanolamine and 1,2-propanediol. This process provides a growth advantage to *Salmonella* enabling it to outgrow other gut flora thereby enhancing dissemination [42–44]. Although less studied, the Grp MCP which is found in some pathogenic *E. coli*, enables 1,2-propanediol metabolism, which has been associated with pathogenesis in *Salmonella* and *Listeria* [29, 45, 46].

Choline utilization MCPs are also closely associated with human health. The Cut MCP metabolizes choline, deficiencies of which have been linked to numerous diseases including atherosclerosis and breast cancer [47, 48]. The Cut MCP is a major source of TMA in the gut, which upon exiting the MCP, travels through the bloodstream to the liver where flavin-containing monooxygenase metabolizes it to trimethylamine-N-oxide (TMAO). TMAO is a marker for non-alcoholic fatty liver disease [49, 50], cardiovascular disease [12, 48, 50, 51], kidney disease [52, 53] and diabetes [54, 55] suggesting that MCP-associated metabolism in the gut plays an important role in physical health.

Distribution of the Pdu, Eut, Cut, and Grp MCPs

The Pdu MCP is thought to be particularly important for bacteria in anaerobic environments, such as soil, sediments, and the gut of higher organisms, where 1,2-propanediol is a major product of fucose and rhamnose fermentation [56]. The *pdu* operon is unevenly distributed among many soil-dwelling and enteric bacteria as well as Firmicutes, Actinobacteria,

Deltaproteobacteria, Synergistetes, Fusobacteria, and Spirochaetes [4, 6]. Among the *Salmonella*, growth on 1,2-propanediol in a B_{12}-dependent fashion is nearly universal whereas this ability is uncommon in *E. coli* [57]. Studies suggest that *Salmonella* acquired this ability by horizontal gene transfer after its divergence from *E. coli* [57].

Ethanolamine, which is metabolized by the Eut MCP in an Ado-B_{12}-depdendent manner, is a component of cellular phospholipids and is present as a free compound within bodily fluids [58]. The *eut* operon is found with high frequency throughout *E. coli* and *Salmonella* [39, 57] (Table 1). It is also located in a variety of other bacterial classes, including Firmicutes, Actinobacteria, Synergistetes, Fusobacteria, and Cloroflexi [4].

Choline, which is common in the diet of animals, is a necessary nutrient for humans and a growth substrate for varied gut bacteria. Because the Cut MCP employs an oxygen-sensitive glycyl-radical enzyme, these MCPs occur exclusively in anaerobic and facultatively anaerobic bacteria. The *cut* operon appears narrowly distributed within the Gammaproteobacteria, but surprisingly it is not found in Bacteroidetes, the largest class of gut-associated bacteria [59]. *Cut* operons have also been identified in Firmicutes, Actinobacteria, and Deltaproteobacteria [4]. Evaluation of the *E. coli* reference collection (ECOR), 72 isolates representing the diversity of the species [60], identified five strains (~7% of the isolates) that were able to degrade choline and contained *cut* genes [30]. In a related survey of gut metagenomic DNA, *cutC* genes were identified in 6.1% of *E. coli* tested [59], suggesting a narrow but important distribution of Cut MCPs. However, *cut* genes have not been found in *Salmonella*.

The Grp MCP, like the Pdu MCP, processes 1,2-propanediol, but is less widely distributed. Grp MCPs are found only in Gammaproteobacteria and Firmicutes [4]. Like the Cut MCP, it relies on an oxygen-sensitive glycyl radical enzyme, and is only found within anaerobes and facultative anaerobes [61]. The ECOR collection was assessed and *grp* genes were identified in 10% of the isolates [29], suggesting that the *grp* operon is slightly more widespread than *cut*. Thus far, *grp* operons have not been found in *Salmonella*.

Lastly, we note that among bacteria that contain MCP gene clusters, about 40% contain two or more [5]. Most *Salmonella* contain both *pdu* and *eut* operons (Table 1). By contrast, most *E. coli* contain a *eut* operon and a small percentage contain *pdu*, *cut,* or *grp* operons, but these latter three have not been found to co-occur. Whether certain *E. coli* strains utilize B_{12}-dependent or -independent 1,2-propanediol degradation is probably dependent on the environments encountered.

MCP operons in *E. coli* and *Salmonella*: an overview

Below, we provide a synopsis of the four major MCPs characterized in *E. coli* and *Salmonella*, including general characteristics, operon layout, and regulation. Further details on structural and genetic studies are presented in the following sections on individual MCP components.

Pdu MCPs

The Pdu MCP of *S. enterica* Serovar Typhimurium LT2 was the first metabolosome discovered and it is the best understood. Pdu MCPs are used for Ado-B_{12}-dependent growth of *S. enterica* on 1,2-propanediol under aerobic or fermentative conditions [62, 63]. In addition, the Pdu MCP supports anaerobic respiration of 1,2-propanediol with tetrathionate as a terminal electron acceptor but not with other acceptors including nitrate, dimethyl sulfoxide (DMSO), TMAO, and fumarate [63]. *S. enterica* synthesizes the Ado-B_{12} needed for 1,2-propanediol metabolism *de novo* under anaerobic conditions but requires added vitamin B_{12} (or another complex precursor of Ado-B_{12}) for aerobic 1,2-propanediol breakdown [10]. A few strains of *E. coli* are able to degrade 1,2-propanediol in a B_{12}-dependent manner, but B_{12}-independent degradation is employed with higher frequency [4].

Figure 2 shows the accepted model of 1,2-propanediol catabolism by *S. enterica*. First, 1,2-propanediol diffuses across the MCP shell and is converted to the toxic intermediate propionaldehyde by an Ado-B_{12}-dependent diol dehydratase (DDH, PduCDE) [22, 64, 65]. The PduQ alcohol dehydrogenase converts propionaldehyde to 1-propanol which exits the MCP and then leaves the cell [66]. Propionaldehyde is also converted to propionyl-phosphate by aldehyde dehydrogenase (PduP) and phosphotransacylase (PduL) [67, 68]. Propionyl-phosphate exits the MCP and is converted to propionate by propionate kinase (PduW) generating 1 ATP [69]. Under respiratory conditions, propionyl-phosphate is thought to be converted back to propionyl-CoA (in the cytoplasm) and feed into the methylcitrate pathway [70]. Within the Pdu MCP, NAD^+ and coenzyme A (CoA) are recycled by the PduQ propanol dehydrogenase and the PduL phosphotransacylase, respectively. Ado-B_{12} (which is subject to breakdown during catalysis) is recycled by the PduGH reactivase, PduS cobalamin reductase, and the PduO ATP-cob(I)alamin adenosyltransferase (ACAT) [71–73]. As mentioned above, the main function of the Pdu MCP is to prevent propionaldehyde toxicity during growth on 1,2-propanediol [31, 32], which presumably is achieved by balancing the rate of propionaldehyde production and consumption by MCP enzymes.

The genes for 1,2-propanediol utilization are found in the *pdu* locus [22]. The main *pdu* operon contains genes for the MCP shell (*pduA, pduB, pduB', pduJ, pduK, pduN, pduT, pduU*); the 1,2-propanediol degradative pathway (*pduCDE, pduL, pduP, pduQ, pduW*); Ado-B_{12} recycling and assimilation (*pduGH, pduO, pduS*); and two genes of uncertain function (*pduM, pduV*) which may be involved in MCP assembly (*pduM*) and MCP segregation at cell division (*pduV*) [22, 64, 67, 74–78]. At the end of the *pdu* operon is a gene (*pduX*) which encodes an L-threonine kinase used for the assimilation of complex precursors of Ado-B_{12} [79, 80]. The *pdu* locus also includes a regulatory protein (*pocR*) and a 1,2-propanediol diffusion facilitator (*pduF*) that are divergently transcribed from the main operon.

In *S. enterica*, the genes of the *pdu* locus are co-regulated with the adjacent B_{12} (cobalamin, *cob*) biosynthetic genes. Both genes sets are induced by PocR in response to 1,2-propanediol [81, 82]. This makes sense as Ado-B_{12} is the required cofactor for the DDH that catalyzes the first step of 1,2-propanediol metabolism [10]. *pdu* genes are also controlled by the global regulators CRP/cAMP, ArcA/B, CsrA, and Fnr [83–86]. CRP/cAMP are needed for

induction the *pdu* genes under both aerobic and anaerobic conditions [83]. ArcA/B, which monitors oxygen availability, further stimulates induction under anaerobic conditions [83, 84]. Transcriptomic studies suggest CsrA is also needed for induction of the *pdu* operon during aerobic growth and proteomics analysis suggest Fnr represses the *pdu* operon in the absence of oxygen [85, 86].

Eut MCPs

The *eut* operon was first identified in *S. enterica* and encodes a bacterial MCP that mediates AdoC-B$_{12}$-dependent ethanolamine catabolism [10, 23, 87, 88]. Under aerobic conditions, ethanolamine acts as a sole source of carbon, energy, and nitrogen [87]. Under fermentative conditions, ethanolamine provides a sole nitrogen source and stimulates growth by providing additional source of ATP [63]. In the absence of oxygen, ethanolamine can also be respired with tetrathionate as a terminal electron acceptor, but better known terminal electron acceptors such as nitrate, DMSO, TMAO and fumarate have not been shown to support ethanolamine respiration [63]. *S. enterica* synthesizes the Ado-B$_{12}$ needed for ethanolamine metabolism *de novo* under anaerobic conditions but requires a complex precursor under aerobic conditions [10, 87, 89]. *E. coli* is unable to synthesize Ado-B$_{12}$ *de novo* and requires a source of complex precursors such as cobinamide or vitamin B$_{12}$ to grow on ethanolamine [57].

The most widely accepted model for the metabolism of ethanolamine begins with its diffusion into the lumen of the Eut MCP [23, 90]. There, ethanolamine is converted to acetaldehyde and ammonia by Ado-B$_{12}$-dependent ethanolamine ammonia-lyase (EAL, EutBC) [91]. Subsequently, acetaldehyde is metabolized by a pathway that is analogous to that employed for propionaldehyde degradation by the Pdu MCP. The EutE aldehyde dehydrogenase, the EutG phosphotransacetylase and the EutD alcohol dehydrogenase convert acetaldehyde to ethanol and acetyl-phosphate [23, 33, 34, 88, 92]. Ethanol exits the MCP and then the cell. Acetyl-phosphate leaves the MCP and is converted to acetate which is excreted into the environment. Under fermentative conditions, this pathway produces 1 ATP, provides a source of nitrogen, and stimulates growth but does not produce a source of cell carbon [63]. Under respiratory conditions, acetyl-CoA generated by ethanolamine catabolism supports growth via the TCA cycle and glyoxylate shunt. NAD$^+$ and HS-CoA are thought to be recycled internally within the Eut MCP by the EutG alcohol dehydrogenase and EutD phosphotransacetylase similarly to the process described above for the Pdu MCP [93]. Ado-B$_{12}$ is also thought to be recycled within the Eut MCP by the EutA reactivase and the EutT ACAT which are unrelated to the B$_{12}$ recycling enzymes of the Pdu MCP [94–97]. Studies indicate that the function of the Eut MCP is to sequester acetaldehyde production to minimize toxicity and prevent carbon loss, as described in more detail above [32–34].

The 17-gene *eut* operon has been characterized mainly in *S. enterica* [23, 33, 34, 98]. Ado-B$_{12}$-dependent EAL is encoded by the *eutBC* genes [99, 100]. Aldehyde dehydrogenase, alcohol dehydrogenase, and phosphotransacetylase enzymes are specified by *eutE*, *eutG*, and *eutD*, respectively [33, 34, 88, 92, 93, 101]. The enzymes used for Ado-B$_{12}$ recycling are encoded by *eutA* and *eutT* [94–97, 102] The *eut* operon contains genes for five shell proteins: *eutS, eutM, eutN, eutK, eutL,* and a putative chaperone, *eutJ*, whose role in MCP

metabolism is unknown [23, 103]. Genes for additional proteins, including two novel acetate kinases (*eutQ, eutP*), a transcriptional regulator (*eutR*), and an ethanolamine permease (*eutH*) round out the operon. The EutQ acetate kinase is required for anaerobic respiration of ethanolamine with tetrathionate, but a specialized role for EutP is not currently known [102]. The EutH permease is most important at lower pH or low external ethanolamine concentrations where it mediates transport of protonated ethanolamine [104]. EutR regulates *eut* transcription in the presence of both ethanolamine and Ado-B$_{12}$ (the required cofactor for ethanolamine ammonia lyase) [87, 105]. EutR also induces its own expression by a positive feedback loop and this is thought to help it compete with EAL for available Ado-B$_{12}$ [106]. In *Salmonella*, the *eut* operon is globally regulated by CRP/cAMP, ArcA/B, and CsrA [107, 108]. In other organisms, regulation of the Eut MCP does not involve EutR and instead employs an unusual noncoding RNA riboswitch [11].

As described above, a number of studies on *eut* regulation were conducted in *S. enterica*. However, *S. enterica* contains both *eut* and *pdu* operons raising the question of how their regulation is coordinated, since essential shell components are highly similar between these two MCPs. *In vivo* studies in *S. enterica* showed that 1,2-propanediol induces the *pdu* operon but acts as a repressor of the *eut* operon, thereby preventing detrimental mixing of the two systems [109]. Therefore, while it is technically possible for MCPs to incorporate non-native components [109–111] leading to some interesting protein design experiments, local regulation may be designed to prevent this in native hosts. We also point out that 40% of bacteria that produce MCPs make two or more; hence, coordinating their expression is broadly important to cell physiology.

Cut MCPs

Craciun and Balskus identified a glycyl radical choline TMA lyase in *D. desulfuricans* and other gut bacteria that converts choline to acetaldehyde and TMA via novel C-N cleavage mechanism [112]. Studies also found that the gene for choline-TMA lyase (*cutC*) clusters with MCP shell protein genes, suggesting this enzyme is MCP-associated [59, 112]. Microcompartment formation linked to choline fermentation was later demonstrated in *P. mirabilis* [28] and subsequently in *E. coli* 536 [30].

In *E. coli* 536, choline stimulates anaerobic growth in media supplemented with a usable carbon source such as yeast extract or fumarate [30]. Although fumarate can function as a terminal electron acceptor for anaerobic respiration by *E. coli*, it is inconclusive whether it does so with choline. *E. coli* is not known to use choline as a nitrogen source suggesting TMA is simply excreted. The Cut MCP does not support aerobic growth presumably because of the extreme oxygen sensitivity of the CutC choline TMA lyase. In *P. mirabilus*, choline supplementation is associated with colony expansion and biofilm formation, but *E. coli* has not been tested for these phenotypes [28]. The Cut MCP has not been identified in *Salmonella*.

The first step of the proposed choline degradation pathway is the conversion of choline to acetaldehyde and TMA within the lumen of the Cut MCP [112]. This reaction is catalyzed by a glycyl radical choline-TMA lyase (CutC) which must first be activated by CutD [30, 112]. It is thought that TMA is excreted and acetaldehyde is converted to ethanol and acetyl-

phosphate as in the Eut MCP [28, 30, 59]. Ethanol is proposed to diffuse out of the MCP into the cytoplasm then out of the cell. Acetyl-phosphate is thought to exit the MCP into the cytoplasm where it is converted to acetate with the generation of 1 ATP. Although this pathway provides ATP, it does not provide a source of cell carbon. Hence, choline stimulates growth of *E. coli* only in media supplemented with a usable carbon source [30]. Based on analogy with the Pdu and Eut MCPs, the Cut MCP is proposed to mitigate acetaldehyde toxicity and carbon loss.

The choline-utilization MCPs are subdivided into two classes (type 1 and type 2) which have substantial differences in distribution and composition [7, 59]. Gene clusters for type 1 Cut MCPs are found in obligate anaerobes and contain 20 genes, while type 2 loci are found in facultative anaerobes and contain 16 genes within two operons. These two classes also have lyases that differ in primary structure. Type 2 CutC enzymes contain an extended ~350 residue N-terminus relative to type 1 lyases which has been suggested to contribute to enzyme activity and/or play a role in targeting CutC to the MCP lumen [7, 113]. *E. coli* strains that metabolize choline contain type 2 Cut MCPs.

In uropathogenic *E. coli* 536, the *cut* locus is located within a pathogenicity island PAI-II$_{536}$ [30, 114]. Here, as is typical for type 2 clusters, there are two operons: the *cutWXY* operon and a "main" *cut* operon separated by an ~519 bp intergenic region (Figure 1). Within the main *cut* operon, *cutC* codes for the glycyl radical choline TMA lyase and *cutD* codes for its partner activating enzyme. It also contains genes for downstream pathway enzymes, including an aldehyde dehydrogenase (*cutF*), alcohol dehydrogenase (*cutO*), and phosphotransacetylase (*cutH*), which were inferred by homology to enzymes found in the Pdu and Eut MCPs, and likely convert the acetaldehyde to ethanol and acetate (Figure 2). Similar to the Eut and Pdu MCPs, it is thought that NAD$^+$ and HS-CoA are recycled internally within the Cut MCP, but conclusive experimental support is lacking [30]. At the end of the *cut* operon are the genes *cutU* and *cutV* which are homologs of efflux pumps that may be involved in product export or substrate uptake, but this has not been reported experimentally. The *cut* locus encodes five shell proteins: *cmcA, cmcB, cmcC, cmcD*, and *cmcE*; however, these do not include a trimeric BMC shell protein related to those found in the majority of MCP operons and hypothesized to transport larger metabolites and enzymatic cofactors through MCP shells [30]. This unexpected finding raises the question of how larger compounds traverse the MCP shell. The presence of the CutU and CutV efflux pumps offers a possible solution.

The Cut microcompartment contains a potentially unique local regulation system that utilizes three proposed regulatory genes (*cutWXY*) located in a operon adjacent to the main *cut* cluster (Figure 1) [30]. Deletions of individual genes showed that *cutX*, which contains sequence similarity to transcriptional regulators, and *cutY*, which does not, are necessary for induction of the *cut* operon by choline. On the other hand, deletion of the *cutW* gene, which encodes a protein with a DNA-binding domain, did not affect *cut* operon induction and its function is currently unknown.

Grp MCPs

The Grp MCP processes the same substrate as the Pdu MCP: 1,2-propanediol. In contrast to the Pdu MCP, the Grp MCP employs a B_{12}-independent glycyl radical diol dehydratase (GR-DDH, GrpM) in the first catabolic step [6, 29, 61]. GR-DDH is extremely oxygen sensitive and the metabolism of 1,2-propanediol by the Grp MCP only occurs under strict anaerobic conditions. In *E. coli* CFT073, the anaerobic metabolism of 1,2-propanediol by the Grp MCP stimulates growth if a source of cell carbon such as yeast extract or fumarate is also present but 1,2-propanediol does not serve as a sole carbon and energy source [29]. Similar to the *cut* operon, 1,2-propanediol was not respired when DMSO, TMAO, or nitrate were provided as terminal electron acceptors [29].

The proposed model for 1,2-propanediol metabolism by the Grp MCP is similar to the model for the Pdu MCP but with GR-DDH (which requires activation by GrpN) replacing B_{12}-dependent DDH in the first catabolic step, the conversion 1,2-propanediol to propionaldehyde [29, 115]. From there, the downstream steps of the pathway that convert propionaldehyde to 1-propanol and propionic acid are thought to be directly analogous to the Pdu MCP. Cofactors are thought to be recycled within the Grp MCP as described for the Pdu MCP, but more supporting work is needed [29]. While the function of the Grp MCP has not been studied, it is presumed to sequester propionaldehyde to mitigate its toxicity.

The *grp* operon has been genetically characterized in uropathogenic *E. coli* CFT073 [29]. The *grp* locus contains 21 genes that encode six pathway enzymes (*grpA, grpB, grpG, grpJ, grpM, grpN*), five shell proteins (*grpE, grpH, grpI, grpK, grpS*), two regulators (*grpP, grpQ*), a permease (*grpO*), and several proteins of unknown function (*grpC, grpD, grpF, grpL, grpR, mrtA, mrtB*). Sequence homology to other MCP components suggests that *grpC* encodes a protein that resembles EutJ, a chaperone of unknown function, while *grpD, grpF, grpL, grpR* encode proteins with homology to a putative flavoprotein, heme-binding protein, protease, and methionine adenosyltransferase, respectively. The *grp* cluster contains three large IGRs (284–549 bp) which is unusual for bacterial gene clusters. Two of these IGRs may be remnants of the horizontal gene transfer because they flank two reverse transcriptase maturase genes (*mrtAB*) which are not involved in 1,2-propanediol metabolism. However, these IGRs might also be involved in gene regulation.

The Grp MCP has been classified as a type 3 glycyl radical microcompartment (GRM 3) [7]. It is distinguished from other classes of GRMs by the substrate processed, gene content of its encoding operon, and protein phylogeny. Additionally, in type 3 GRMs, GR-DDH contains a 50–60 residue region between its two structural domains which may be involved in enzyme localization to the MCP lumen.

Regulatory studies found that the *grp* operon in *E. coli* CFT073 is induced by 1,2-propanediol and is regulated by a two-component regulatory system, *grpP* (histidine kinase) and *grpQ* (response regulator), located near the end of the operon [29]. Related studies in *R. capsulatus* also identified a similar regulatory pair, pointing out partial sequence conservation with PocR which regulates the *pdu* operon in response to 1,2-propanediol [115]. The operon organization of *R. capsulatus* differs from *E. coli* CFT073 and other identified GRMs. In most GRMs, the gene for the activating enzyme is adjacent to the GRE,

possibly indicating co-regulation. However, these two components are located near opposite ends of the operon in *R. capsulatus* [115]. Whether this difference affects enzyme activation and function is unknown.

Main components of MCPs

Targeting sequences

The question of how cargo is directed to the MCP interior during assembly is essential to a complete understanding of these organelles. An early clue regarding MCP assembly came from bioinformatic studies that identified terminal extensions of roughly 20 amino acids present on a subset of MCP proteins but absent from homologs that are not MCP associated [116]. Subsequent genetic and biochemical work showed that a number of such extensions (referred to throughout the literature as 'signal sequences', 'targeting sequences', or 'encapsulation peptides') were necessary and sufficient for directing enzymes to the lumen of bacterial MCPs. Functional N-terminal targeting sequences were demonstrated for DDH (PduCDE) [117] and EAL (EutC) [118] as well as two MCP-associated aldehyde dehydrogenases (PduP and EutE) [119, 120]. In addition, bioinformatic studies indicated that targeting sequences are widely used for the encapsulation of proteins into diverse MCPs, and share a similar pattern of alternating polar and hydrophobic residues, although their sequences are poorly conserved [110, 121, 122]. An NMR structure of the 18-residue N-terminal targeting sequence of PduP revealed that this region forms an amphipathic helix [123], and it was suggested that other targeting sequences adopt a similar fold. Due to their widespread and generic character, targeting sequences do not appear to be overly specific for particular MCPs. In fact, targeting sequences from varied MCPs as well as non-native sequences are able to direct enzymes to the Pdu MCP simply through a common hydrophobic motif [110]. However, many MCP-associated proteins lack recognizable targeting sequences, indicating that other mechanisms are also used to facilitate assembly and encapsulation [116, 121].

How targeting sequencing mediate encapsulation of MCP core enzymes and participate in shell assembly is not fully understood. Presumably, targeting sequences bind MCP shell proteins to mediate encapsulation during assembly. Supporting this idea, studies indicate that targeting sequences found on Eut and Pdu enzymes bind to the PduA, PduJ, PduK, and EutS shell proteins [103, 116, 123]. Furthermore, in the case of the PduP aldehyde dehydrogenase, evidence indicates that its N-terminal targeting sequence binds to the C-terminal helix of PduA and PduJ. Recent work suggests that PduP is still trafficked to the MCP shell in the absence of PduA, indicating that multiple partner proteins may be involved in binding cargo to the protein shell [124]. The interplay between shell proteins and shell contents remains an important, yet underexplored area of MCP research.

Signature Enzymes

Enzymes that determine MCP substrates are sometimes referred to as signature enzymes. With regard to the MCPs found in *E. coli* and *Salmonella*, the signature enzymes are the PduCDE Ado-B_{12}-dependent diol dehydratase (DDH) of the Pdu MCP, the EutBC Ado-B_{12}-dependent ethanolamine ammonia lyase (EAL) of the Eut MCP, the CutC glycyl radical

choline TMA lyase of the Cut MCP, and the GrpM glycyl radical diol dehydratase (GR-DDH) of the Grp MCP. In each of these cases, the signature enzyme catalyzes the first step of substrate breakdown.

B_{12} Dependent Enzymes—Ado-B_{12}-dependent ethanolamine ammonia lyase (EAL) in the *eut* system and diol dehydratase (DDH) in the *pdu* system catalyze the first steps of ethanolamine and 1,2-propanediol degradation, respectively [23, 64, 88]. While there are distinguishing features between these two enzymes, they both utilize the same basic mechanism [125]. These enzymes use Ado-B_{12} in the "base-on" form, meaning that the dimethylbenzimidizole (DMB) ring is coordinated to the central cobalt atom [126]. Binding coenzyme B_{12} by the apoenzyme allows for activation through homolytic cleavage of the Co-C bond creating cob(II)alamin and the 5'-deoxyadenosyl radical. Binding substrate shifts the equilibrium toward activation from 1% to 60% and 90% for DDH and EAL, respectively [127]. The generalized reaction mechanism is as follows: the adenosyl radical abstracts a hydrogen from the substrate, the substrate radical rearranges to form the product radical, which abstracts a hydrogen from 5'-deoxyadenosine, allowing cob(II)alamin and the adenosyl radical to recombine and regenerate the starting state of the enzyme.

B_{12} Dependent Enzyme Reactivases—Both EAL and DDH are subject to substrate-dependent and substrate-independent inactivation by the formation of catalytically inactive forms of cobalamin [125, 128]. In the case of substrate-independent inactivation, O_2 reacts with activated enzyme forming HO-B_{12} which remains tightly bound in the active site [129]. In substrate and substrate analog inactivation, 5'-deoxyadenosine and a catalytically inactive cobalamin is formed and degraded to HO-B_{12} [130–132]. The reactivation of enzyme and recycling of the HO-B_{12} to Ado-$B_{12}$is understood to be handled inside the MCP by MCP-associated proteins. The reactivase mechanism has been heavily studied in both Pdu and Eut and is the subject of detailed reviews [125, 133]; here we briefly highlight the key steps. Removal of HO-B_{12} is mediated by PduGH or EutA reactivases in the relevant MCPs, both of which require ATP and Mg^{2+} [96, 134]. The PduGH structure in *K. oxytoca* was solved by X-ray crystallography, and homology analysis identified similarity to the ATPase domain of the *E. coli* HSP70 DnaK, suggesting it may function as a chaperone that partly unfolds DDH releasing HO-B_{12} [135]. After release from the inactive enzyme, HO-B_{12} is converted back to Ado-B_{12}. This begins with reduction of HO-B_{12} to cob(I)alamin by the PduS cobalamin reductase in the case of the Pdu MCP or by an unknown means in the case of the Eut MCP [71, 136]. Cob(I)alamin is adenosylated to form Ado-B_{12} by the PduO [72, 128] or by the EutT ACAT [94, 95] in a reaction where ATP is the adenosyl-group donor. Lastly, Ado-B_{12} reassociates with DDH or EAL apoenzymes to form active holoenzyme, completing the reactivation cycle. In *S. enterica*, deletion of PduS cobalamin reductase partly impairs 1,2-propanediol degradation [71]. This may be due to functional redundancy with NAD(P)H:Flavin oxidoreductase (Fre) or $NADP^+$:ferredoxin(flavodoxin) reductase (Fpr) [137, 138], although genetic analyses have not yet fully worked this out. Deletion of the PduO or EutT ACAT partially impairs 1,2-propanediol or ethanolamine degradation, respectively [72, 95]. Both enzymes are thought to be partially redundant with the CobA housekeeping ACAT since *cobA eutT* or *cobA pduO* double mutants are unable to grow on ethanolamine or 1,2-propanediol, respectively [72, 94, 95]. Presumably, the PduO and EutT

ACATs are more efficient at recycling Ado-B_{12} internally within their respective MCPs, but experimental evidence for this has not yet been reported.

Ethanolamine Ammonia Lyase (EAL, EutBC)—While the overall mechanism is the same for both EAL and DDH, the substrate specificity and structure of these two enzymes are not. EAL (PDB: 3ABO, crystal structure from *E. coli* K-12 [91]) is composed of two subunits (EutB and EutC) that come together as a dodecameric ring $(\alpha_2\beta_2)_3$. Using modelling and validated by biochemical methods, Bovell and Warncke put forward a model of assembly where EutB dimerizes and then trimerizes to form a EutB hexameric ring allowing EutC to dimerize with EutB to form the final $[(EutB\text{-}EutC)_2]_3$ complex [139]. The Ado-B_{12} is sandwiched between the EutB and EutC subunits, oriented with the DMB liganded face toward EutC [91]. Genetic knockout studies have shown that mutants lacking *eutBC* are unable to grow on ethanolamine [33, 88]. Studies indicate that the EutC subunit of EAL has a functional targeting sequence that presumably directs its encapsulation into the Eut MCP [118].

Diol Dehydratase (DDH, PduCDE)—In *Salmonella*, three genes encode the diol dehydratase encapsulated in the Pdu MCP (PduCDE) [64]. Unlike EAL, which makes a trimer of dimers, PduCDE from *Klebsiella oxytoca* (96% amino acid similarity to *Salmonella* PduCDE) forms a dimer of trimers $(\alpha\beta\gamma)_2$ where PduC makes up the full dimer interface and PduD and PduE are on opposite sides of PduC from the dimer interface [140]. Both PduD and PduE have N-terminal extensions compared to homologs that are not MCP associated; however, only the N-terminal extension of PduD been shown to function as a targeting sequence [117]. A number of *in vivo* and *in vitro* studies established that PduCDE localizes to the lumen of the Pdu MCP [22, 78, 117, 141], and knockouts of PduCDE abolish 1,2-propanediol metabolism by *Salmonella* [73].

Glycyl Radical Enzymes (GREs)—A widespread, but less well-studied class of MCPs (which includes the Cut and Grp MCPs of *E. coli*) uses glycyl radical enzymes to initiate substrate metabolism. These enzymes employ a glycyl radical instead of an 5'-deoxyadenosyl radical generated from Ado-B_{12} for catalysis [142, 143]. GREs, unlike B_{12}-dependent enzymes, need to be initially activated by a radical S-adenosylmethionine (SAM) enzyme [142]. Each GRE has a specific partner activating enzyme (AE) [144]. The AE generates a 5'-deoxyadenosyl radical (from SAM) which abstracts a hydrogen from the active site glycine in the GRE. In the presence of substrate, the glycyl radical abstracts a hydrogen from a nearby cysteine generating a thiyl radical. The thiyl radical abstracts a hydrogen from the substrate to form the substrate radical allowing for radical rearrangement to produce the product radical. At this point the thiyl radical is regenerated, producing the final product, and lastly the glycyl radical is regenerated [143]. While the AE is necessary, it is only needed for initial activation, after which the catalytic cycle regenerates the glycyl radical. The glycyl radical is extremely oxygen sensitive and can react with molecular oxygen, cleaving the peptide backbone at the site of the radical. In *E. coli*, GRE "spare parts" proteins have been identified, which will replace the portion of enzyme missing after O_2 inactivation [145], but these are not encoded within the MCP operons.

CutC (a type 2 lyase) is the only microcompartment GRE characterized in detail [7, 112, 113, 146]. Crystal structures of CutC from *K. pneumonia*, were determined in both the presence and absence of choline substrate, revealing an unexpected topological change upon choline binding [113, 147], in contrast to other non-MCP associated GREs. As expected, deletion of either the choline TMA lyase gene (*cutC*) or the gene for its activating enzyme (*cutD*) eliminates choline degradation by the Cut MCP [30]. Similarly, deletion of GR-DDH (*grpM*) or its activating enzyme (*grpN*) prevent 1,2-propanediol metabolism by the Grp MCP [29].

MCP Pathway Enzymes

In the Pdu, Eut, Cut, and Grp MCPs discussed here, the signature enzyme generates an aldehyde (acetaldehyde or propionaldehyde) product which is metabolized to the corresponding alcohol and organic acid by a conserved pathway using the enzymes described below (Figure 2).

Aldehyde dehydrogenase—Aldehyde dehydrogenases (Ald) are used for substrate metabolism by the Pdu, Eut, Cut, and Grp MCPs. These enzymes convert an aldehyde, HS-CoA, and NAD^+ to and the corresponding acyl-CoA and NADH internally within MCPs. Aldehyde dehydrogenases are essential to functional MCPs; when the *pduP, eutE, cutF* or *grpJ* aldehyde dehydrogenase genes are individually deleted, growth on the respective substrates is eliminated [29, 30, 67, 88]. *In vitro* assays of purified enzyme verify that PduP and EutE have Co-A-acylating aldehyde dehydrogenase activity [92]. The PduP and EutE aldehyde dehydrogenases were shown to have N-terminal targeting sequences that mediate their encapsulation into the Pdu and Eut MCPs [93, 116]. In addition, PduP was shown to co-purify with Pdu MCPs [67, 119] and a series of genetics studies localized EutE to the interior of the Eut MCP [93]. CutF and GrpJ also have aldehyde dehydrogenase activities as shown by *in vivo* assays, and a structure of GrpJ from *Rhodopseudomonas palustrius* has been solved [30, 61]. Like their EutE and PduP counterparts, the CutF, and GrpJ aldehyde dehydrogenases have N-terminal extensions predicted to mediate MCP encapsulation, but experimental support for this function has not been reported.

Phosphotransacetylase—Nearly all metabolosome operons encode phosphotransacylase (PATC) enzymes or homologs thereof. Within the metabolosome, PATC enzymes accept the acyl-CoA products of aldehyde dehydrogenases and convert them to acyl-phosphates and HS-CoA [68, 75]. This not only produces a high-energy phosphate compound, it regenerates HS-CoA for the aldehyde dehydrogenases. Genetic deletion of the PATC genes found in the *pdu, eut, cut*, and *grp* operons results in partial growth impairment under standard growth conditions, and in the case of *eut*, no growth under stringent conditions [29, 30, 75, 93]. The explanation for these phenotypes is that MCP-associated PATC enzymes have activities that are redundant with housekeeping enzymes, but are still needed for regenerating HS-CoA internally within the MCP. Fairly extensive genetic studies on both the PduL and EutD PATC enzymes supports a role in internal cofactor recycling; the key finding being that breaking the MCP shell corrects the phenotypes of PATC deletions [75, 93]. Both PduL and EutD have been recombinantly expressed and purified, and biochemical assays verify that they possess PATC activity [75, 148]. The PduL class of

PATC, which is the most common version encoded by MCP operons, is unrelated in sequence to the housekeeping enzymes (Pta) which are widespread in biology. The crystal structure of PduL from *Rhodopseudomonas palustris* has been solved, and it forms a dimer in the crystals, as well as by SEC. However, Phe116, which is important for dimerization, is poorly conserved, and is not present in *S. enterica* PduL. This brings into question the oligomeric state of PduL generally [149]. The EutD enzyme of *S. enterica* is related in sequence to the C-terminal PTA_PTB domain of housekeeping Pta enzymes [101] and is less common in MCP operons compared to PduL-type PATC enzymes. The PTAC enzymes in the *cut* and *grp* operons (CutH, GrpB) which are PduL-type have not been assessed in any detail. However, deletion of their encoding genes results in partial impairment of growth consistent with a role in internal cofactor recycling [29, 30].

Acetate/propionate Kinase—Acetate/propionate kinases are often encoded by MCP operons but are thought to localize to the cytoplasm of the cell rather than the MCP interior. These enzymes catalyze the conversion of an acyl-phosphate, ADP, and Pi to the corresponding organic acid and ATP. The *eut* operon encodes two acetate kinases (EutP and EutQ). Both show activity *in vitro*. EutQ is necessary for growth of *S. enterica* on ethanolamine under anoxic conditions, while EutP deletions have no known phenotype [97]. The analogous Pdu protein PduW shows propionate kinase activity and catalyzes the conversion of propionyl-phosphate to propionate with the production of ATP from ADP and Pi [69]. However, PduW is not necessary for growth on 1,2-propanediol under any tested condition. This suggests that PduW is functionally redundant with the housekeeping acetate kinase (Ack) [69]. Presumably, PduW contributes the degradation of 1,2-propanediol under as of yet unidentified conditions. The type 2 *cut* operon of *E. coli* 536 is not known to contain an acetate kinase and likely relies on the housekeeping Ack enzyme for this function [7]. For the Grp MCP, *grpG* is believed to be a propionate kinase by homology, and knocking out *grpG* partially impairs growth on 1,2-propanediol [29]. This suggests that GrpG might have an MCP-specific role, but the details are unclear.

Alcohol dehydrogenase—Most MCP operons encode alcohol dehydrogenases (or homologs) that convert aldehydes and NADH to alcohols and NAD$^+$. The primary function of these enzymes in MCP metabolism is to regenerate NAD$^+$ from NADH (formed by the aldehyde dehydrogenase reaction) internally within the MCP [66, 75, 93]. Deletion of MCP-associated alcohol dehydrogenases typically only partially impairs growth due to functional redundancy with housekeeping enzymes under fermentative conditions or the electron transport chain under respiratory conditions. Internal NAD$^+$ recycling by MCP alcohol dehydrogenases is well-supported by genetic studies on both the Eut [93] and Pdu [66] MCPs. The alcohol dehydrogenases encoded by the *cut* and *grp* operons have not been as extensively studied. However, genetic deletion of the *cutO* or *grpA* alcohol dehydrogenase partially impaired substrate metabolism suggesting a role in NAD$^+$ recycling as well as partial redundancy with housekeeping Adh enzymes [29, 30]. Above, we mentioned genetic analyses that indicated functional redundancy between MCP-associated alcohol dehydrogenases and housekeeping Adh enzymes or the electron transport chain. However, regenerating NAD$^+$ outside the MCP for use within the MCP requires that NADH and NAD

+ move across the MCP shell, by a means that has not been defined, but which may involve gated channels in trimeric shell proteins as described further below.

Microcompartment Shell Proteins

The outer boundary of bacterial MCPs is a polyhedral protein shell 100–400 nm in diameter, which is similar in morphology across the MCPs considered here [29, 30, 103, 141] (Figure 3). MCP shells form a selectively permeable barrier which allows the passage of substrates and products while sequestering toxic and/or volatile pathway intermediates. Remarkably, the shells of diverse MCPs are built primarily from a single family of small, functionally diversified proteins known as bacterial microcompartment (BMC) domain proteins (Pfam00936) [150]. There are two main groups of BMC domain proteins: hexameric (BMC-H) and trimeric (BMC-T). As the name suggests, BMC-H proteins assemble into hexamers in solution, with each monomer contributing a BMC domain. Each BMC-T monomer, by contrast, is comprised of two fused BMC domains and three monomers assemble into pseudohexameric trimers. Both BMC-H and BMC-T shell proteins share a similar flat hexagonal quaternary structure. MCP shells are typically built from two to ten different types of BMC domain proteins (BMC-H and BMC-T combined) that tile edge-to-edge into mixed sheets, forming the facets of the shell. Variations in BMC domain proteins are thought to allow the metabolism of diverse substrates in a ranges of host organisms [151–153]. The diversification of BMC domain proteins includes circular permutations, [Fe-S] clusters, and fusions to a number of different domains of unknown function [154–157]. In addition to BMC domain proteins, MCPs also contain conserved pentameric proteins that cap the vertices and impart shell curvature. These are known as bacterial MCP vertex proteins (BMV) or BMC-P proteins (Pfam0916) [151–153, 158].

Numerous BMC shell protein structures have been solved by crystallography [2, 9, 151, 153, 155, 159–164]. Together with genetic and biochemical studies, these findings have substantially advanced our understanding of shell assembly and function (Figure 4). In addition, several structures of empty recombinant shells have been reported recently, providing further insights into MCP architecture [147, 165–167]. Below, we provide more detailed information on MCP shells proteins focusing on those from the Pdu, Eut, Cut, and Grp MCPs of *E. coli* and *Salmonella*.

Hexameric Shell Proteins (BMC-H)

Hexameric BMC shell proteins are the most prevalent class, and the *pdu*, *eut*, *cut*, and *grp* loci of *Salmonella* and *E. coli* all encode multiple BMC-H proteins. The structure of BMC-H proteins is highly conserved among diverse MCPs (Figure 4A–B). In crystals, BMC-H proteins are usually flat, hexagonally-shaped cyclic hexamers [159, 168–170] which interact edge-to-edge to form sheets. Two positively charged residues at the hexamer edge, (K26 and R79 in the canonical BMC-H protein PduA) are crucial for hexamer-hexamer tiling and are widely conserved across BMC-H (and BMC-T) proteins, suggesting a common manner of assembly [152, 171–173].

The primary opening in the protein sheets formed by BMC-H proteins is a 5–10 Å diameter pore at the center of each hexamer. Studies indicate that these pores allow the selective

diffusion of small metabolites into and out of MCPs. *In vivo*, *in vitro*, and *in silico* studies showed that the PduA hexamer preferentially allowed the diffusion of 1,2-propanediol (compared to propionaldehyde) across the shell of the Pdu MCP [163, 174]. Although the topology of BMC-H hexamers is highly conserved, the residues lining the pores may vary in their chemical and physical properties suggesting they mediate selective transport of different compounds, presumably MCP substrates and products. This might explain in part why MCP operons often encode multiple BMC-H proteins. For example, altering the chemical properties of the PduA pore residues by site-directed mutagenesis was sufficient to change the permeability of the Pdu MCP [111, 163]. Additionally, both *in vivo* and *in vitro* studies have highlighted the importance of relative gene position in shell function and formation which could also account for multiple BMC-H genes within a single MCP operon [78, 162].

BMC-H proteins are understood to make up a large portion of the microcompartment shell and as a result, play a pivotal role in MCP formation [124, 141, 165]. For the Pdu MCP of *S. enterica*, the PduA and PduJ shell hexamers are estimated to comprise ~40–60% of the protein of the shell [124, 141], and deletion of the *pduA* or *pduJ* genes individually results in the formation of aberrant microcompartments and propionaldehyde toxicity [76]. Similarly, a knockout of the EutM BMC-H component of the Eut MCP causes the buildup of acetaldehyde and cellular toxicity most likely as a result of a defective shell [33]. The effects of BMC-H gene knockouts on the Cut MCP are currently uncertain as relatively limited work has been reported and characteristic phenotypes were not observed [30]. Knockouts of BMC-H protein GrpH (as well as other shell proteins of the Grp MCP) revealed the surprising phenotype of inhibition of growth stimulation by substrate, suggesting that the Grp MCP shell is essential for enzymatic activity *in vivo*, in contrast to other MCPs studied [29].

The *pdu*, *eut*, *cut,* and *grp* operons also contain variations of canonical BMC-H proteins, including circular permutations (found in EutS, PduU, and GrpK) where the quaternary structures of permuted hexamers align well with canonical hexamers but their secondary structural elements are in a different order. A unique feature of some permuted hexamers is an N-terminal extension from each subunit which forms a six-stranded beta barrel "capping" the pore, as first observed in the crystal structure of PduU from *S. enterica* (Figure 4C) [155]. If and how occlusion of the central pore is controlled by pathway flux or interactions with specific metabolites remains unknown.

Another variation on the BMC-H theme are canonical hexamers with C-terminal extensions. At least one copy of this protein type is found in the four operons discussed here (PduK, CmcE, EutK, GrpS). The exact role of these extensions is unknown. In the case of PduK, its C-terminus includes an [Fe-S] cluster binding motif, suggesting a role in electron transfer [7, 155, 157]. Biochemical and structural analyses of EutK show that it does not purify as a hexamer and contains a putative DNA binding domain whose role in shell structure and/or MCP assembly is not known [159]. With regard to CmcE and GrpS, so far there have been no reports on the function of their C-terminal domains. In addition to examples mentioned here, extended BMC-H proteins are widespread among diverse MCPs and warrant further study.

Trimeric Shell Proteins (BMC-T)

BMC-T proteins have a similar topology to BMC-H proteins and are thought to have arisen by gene duplication and divergence of BMC-H proteins. Each BMC-T monomer contains two circularly permuted or two canonical Pfam00936 domains and assembles into trimeric pseudohexamers that have six-fold symmetry [150]. Like BMC-H oligomers, BMC-T trimers contain a central pore region; however, this region may be occluded by an [Fe-S] cluster or may be dynamic, opening and closing in response to environmental conditions. The *pdu, eut,* and *grp* loci of *Salmonella* and *E. coli* all encode BMC-T proteins, but the *cut* locus is unusual in that it does not.

PduB and PduB' are the major BMC-T proteins of the Pdu MCP of *S. enterica*, together comprising about 25–50% of the total shell protein content [124, 141]. PduB and PduB' are permuted trimers transcribed from overlapping genes and are identical in amino acid sequence except that PduB' is shorter by 37 amino acids on the N-terminus. These 37 residues play a key role in assembly of the Pdu MCP. When removed, large MCPs lacking lumen enzymes result, indicating that the N-terminus of PduB is needed for the encapsulation of enzymatic cargo [175]. A crystal structure of PduB from *L. reuteri* (62% sequence similarity to *S. enterica*) displays the major structural hallmarks of BMC-T oligomers, and is discussed in more detail below [161]. *S. enterica* strains with *pduBB'* deletions fail to make MCPs, instead producing polar bodies which are aggregates of other MCP proteins [76]. Such mutations also result in propionaldehyde accumulation, cellular toxicity, and DNA damage during growth of *S. enterica* on 1,2-propanediol.

The Eut operons of *E. coli* and *Salmonella* encodes a single permuted trimeric BMC domain protein, EutL. Interestingly, EutL crystallized in both "open" and "closed" conformations where a 10Å central pore present in the open form is absent in the closed form (Figure 4D–E) [153]. This suggests that EutL may allow selective transport of metabolites to and from the MCP interior through a gating mechanism [159, 160]. In addition to the gated central pore, the crystal structures of EutL revealed allosteric binding pockets between the tandem repeat domains, which could serve to "unlock" the central gate under specific conditions [161, 164]. In a crystal structure of the closed form of EutL from *C. perfringens* (73% sequence similarity to *S. enterica*), ethanolamine was shown to bind in these pockets, presumably as a means of negative allosteric regulation [164]. Glycerol was shown to bind in an similar location in the closed crystal structure of PduB from *L. reuteri,* likely fulfilling the same function in the Pdu system [161]. BMC-T proteins from β-carboxysomes have also been crystallized in open and closed forms. In addition, these trimeric rings have been shown to stack face-to-face, forming a central cavity that might function by an airlock mechanism in metabolite transport [176–178]. A working model suggests that larger metabolites such as ATP or cobalamin could traverse the shell using this method while aldehyde intermediates remain trapped within [164]. However, active gating has not yet been demonstrated *in vivo* or *in vitro*.

Another type of BMC-T protein, exemplified by PduT from the Pdu MCP, is composed of canonical BMC domains but surprisingly contains a [4Fe-4S] cluster blocking the central pore [155, 156] (Figure 4F). This arrangement, coordinated by loops containing conserved Cys residues contributed by each subunit, may function in facilitating redox chemistry such

as regenerating encapsulated cofactors via electron transfer across the microcompartment shell [155]. In a recent study, site-directed mutagenesis of the conserved Cys residues to remove the [Fe-S] clusters (leaving behind pores) resulted in greater diffusion of substrate, intermediate, and NAD^+/NADH cofactors, when small charged or uncharged residues were substituted [179]. These findings indicate that alteration of the pore chemistry is a reasonable method for fine-tuning transport through BMC-T oligomers.

The *grp* locus of *E. coli* CFT073 encodes a single BMC-T protein, GrpI. It is in the permuted class, suggesting a role in dynamic solute transport. Structural characterization of GrpI has not been reported, however, a genetic knockout of *grpI* in *E. coli* CFT073 eliminated growth on 1,2-propanediol [29]. This phenotype was unexpected since shell gene knockouts in other MCPs result in aldehyde toxicity and DNA damage but typically do not prevent growth on MCP substrates.

As mentioned above, the *cut* operon of *E. coli* 536 lacks a BMC-T gene, but this organism is still able to metabolize choline, extrude product, and form MCPs which are similar in size to Pdu MCPs [30]. Other proteins may compensate for the role of BMC-T proteins in this system. Genetic knockouts of *cutU* and *cutV*, putative efflux pumps which might fulfil the function of BMC-T proteins in the Cut MCP, abolish choline metabolism, suggesting a different method of large metabolite transport in this class of B_{12}-independent MCPs. Alternatively, it is possible that other yet uncharacterized elements of the Cut MCP system may be involved in large metabolite transport.

Bacterial MCP vertex (BMV) proteins

Most (or all) MCPs are thought to use proteins with conserved Pfam03319 domains as vertices [151, 158]. BMV proteins generally occur in low abundance in MCPs, since fewer copies relative to other proteins are needed for shell assembly. Because of this, BMV proteins were not initially identified in preparations of purified MCPs [141, 180]. Subsequently, the PduN vertex protein was found to be a component of both purified Pdu MCPs and recombinant empty shells by Western blotting [76] and GFP tagging [78]. More recently, the role of various BMV proteins as vertices was demonstrated when the structures of several empty MCP shells were assigned [147, 165, 167].

Unlike other shell proteins, BMV proteins are pentameric in arrangement. The first BMV proteins to be identified, CcmL and CsoS4A from two types of carboxysomes, were found to be pentamers whose size and shape were compatible with vertex formation [151]. Later GrpN from *R. rubrum* was also shown to form pentamers [158] (Figure 4G). Surprisingly, the BMV protein from the *eut* operon (EutN) crystallized as a hexamer with pseudo-pentameric symmetry [151]. However, additional biochemical studies showed that EutN forms a pentamer in solution, in agreement with other BMV structures [158]. In some instances outside of *E. coli* and *Salmonella*, multiple copies of BMV genes may exist in a single MCP operon [181]. Although the rationale for this diversity has not been determined, it suggests additional roles for BMV proteins beyond capping MCP vertices.

Genetic studies have shown that BMV proteins are essential for proper formation of the Pdu, Eut, Cut, and Grp MCPs. In *S. enterica*, deletion of *pduN* resulted in Pdu MCPs with

unusual shapes by EM as well as propionaldehyde toxicity during growth on 1,2-propanediol [76]. Similarly, increased acetaldehyde accumulation was observed when *eutN* was genetically deleted from the *S. enterica eut* operon, again indicating a role in proper MCP formation [33]. Recent work on the *cut* operon in *K. pneumoniae* revealed that recombinant empty MCP shells were not formed without the *cmcD* pentamer [147]. And finally, in the *grp* operon of *E. coli* CFT073, deletion of the *grpE* gene prevented growth on 1,2-propanediol indicating a role in MCP function [29].

Specifically, if and how vertex proteins are able to impart curved structure to MCPs has been explored computationally, but not experimentally [182, 183]. It is possible that vertex capping occurs as a later step in metabolosome formation, similarly to β-carboxysome assembly [184, 185]. In keeping with this hypothesis, vertex proteins have been utilized in a novel strategy for the purification of synthetic MCPs with a complete shell. By attaching a strep affinity tag to recombinantly produced vertex proteins, MCPs expressed in the absence of BMV proteins may be "sealed" and purified in a single step on an affinity column [186]. Whether this technique can be employed across diverse metabolosomes has not been investigated.

Shell-associated proteins

Some shell-associated proteins are also predicted to play a role in MCP architecture and assembly. Deletion of the *pduM* gene, which lacks a BMC domain, leads to the formation of highly aberrant MCPs and cells that undergo propionaldehyde toxicity during growth on 1,2-propanediol [74]. Similarly, the EutQ acetate kinase (also lacking a BMC domain) is necessary for shell integrity and acetaldehyde degradation under anoxic conditions, but also is able to bind to the N-terminus of the BMC-H protein EutM and increases the cellular copy number of Eut shells by an unknown mechanism [97, 103]. How and when these various interactions occur during MCP assembly is unknown.

Although not well studied, some MCP-associated proteins are predicted to interact with the external face of the shell, providing clues regarding native MCP intercellular localization. PduV, a protein of unknown function with sequence similarity to RAS-type GTPases, was shown by GFP tagging to localize to the external face of empty Pdu MCPs [78]. Additionally, based on its dynamics over time, PduV was speculated to be involved with anchoring MCPs to the cytoskeleton in growing bacterial cells. Further evidence from computational docking studies and bacterial II hybrid experiments predicted an interaction between the N-terminus of PduV and the C-terminal extended β-barrel of PduU, placing PduV on the external face of the MCP [187]; these findings were supported by recent GFP localization studies [124]. Whether other MCP operons also include external shell-associated proteins remains to be determined, although a similar role has been suggested for shell protein PduK [76] and cytoskeletal movement of MCPs has been detected but not localized in Eut [118]. Details of the global spatial organization of MCP-containing cells beyond cytoskeletal attachment has remained elusive due to challenges with electron microscopy visualization [188] and the findings that knockouts of individual MCP genes may produce profound effects on MCP abundance, structure, and assembly [76, 103, 175].

Understanding these complex interactions could provide additional details on MCP function and their specific role in cellular metabolism.

Cryo-EM and Crystal Structures of Empty MCP shells

Recently, recombinant empty MCP shells amenable to crystallography and cryo-EM have been produced in *E. coli* and characterized structurally [147, 165, 167]. The recombinant shells that have been analyzed thus far were composed of a subset of shell proteins and lacked core enzymes, resulting in structures that were much smaller but more homogeneous than wild-type MCPs. It seems reasonable that these structures assembled in a physiologically relevant manner, but studies with native MCPs will be needed to rigorously establish the overall structure with all components present.

A subset of MCP shell proteins was utilized to obtain the first high-resolution structure of an intact empty metabolosome shell from *H. ochraceum* [165, 166]. Mixed sheets of BMC-H and BMC-T proteins formed the facets of the shell which was icosahedral in shape. Interestingly, the permuted BMC-T proteins were arranged into a two-BMC-T stack, presumed to act as an "airlock", potentially allowing tight control of metabolite flux [165, 166]. Additionally, BMV proteins formed the vertices, as anticipated [151, 159]. The global arrangement of proteins forming this shell resembles the cryo-EM structure of an empty β-carboxysome [167], suggesting structural similarities in the overall construction of carboxysomes and metabolosomes. Recently, an empty Cut MCP shell was characterized in *K. pneumoniae* using a subset of shell proteins: CmcABC'D (CmcC' contained an extended C-terminus) [147]. Like other empty shells, the structure was icosahedral and highly regular, although the authors note that including all five native shell proteins from the *cut* operon resulted in larger and less homogeneous shell preparations. To date, a structure of a native MCP (containing cargo) has not been determined; how the structural organization differs from the empty shells would shed light on a number of important questions.

Applications of Bacterial Microcompartments

As more information has been revealed about the structure and function of MCPs, attempts to use this knowledge toward biotechnology applications has also advanced. Diverse MCPs including carboxysomes and metabolosomes have been heterologously expressed in *E. coli* and other organisms, allowing the transfer of MCP functions to new hosts. In addition, these applications have allowed a better understanding of component parts of MCPs and revealed key rules in particle assembly and stability [186, 189–192].

Along these lines, number of groups are working on engineering carboxysomes into C3 plants with the goal of improving CO_2 fixation and reducing photorespiration [2, 191–193]. Additionally, a great deal of effort has also gone into repurposing metabolosomes as enzyme scaffolds, nanobioreactors, containers for toxic proteins, and hybrid enzyme-inorganic catalysts [14–17, 194]. Here, we briefly outline the main research directions in MCP bioengineering, including the design and production of empty protein shells from MCP components, the use of targeting sequences to drive novel cargo encapsulation, efforts to control shell permeability, and repurposing MCPs toward novel functions. For more

information, we refer readers to a number of excellent reviews on this subject [14, 16, 195–198].

"Empty" MCPs and Production in Industrial Hosts

Parsons and colleagues were the first to demonstrate the assembly of a cargo-free MCP shell by developing a fusion plasmid containing all essential shell genes in the *pdu* operon from *C. freundii* and expressing these recombinantly in *E. coli* [78]. Later, empty protein shells from carboxysomes [167], a *Haliangium ochraceum* MCP of unknown function [165], the Eut MCP [103, 118], and the Cut MCP [147] were also produced in *E. coli*. Protein shells have also been assembled *in vitro* from single shell proteins at an oil-water interface [199] and from multiple shell proteins modified with cleavable SUMO tags to block premature assembly of individual shell proteins into protein sheets [186].

Another approach to the production of protein shells has been the redesign of native MCP shell proteins. A circularly permuted variant of PduA was found to form a 60-subunit nanocage [200]. Interestingly, this novel compartment was sensitive to changes in pH and salt concentration; environmental factors which could provide biological tuning for further applications. Also along these lines, empty shells were formed by a synthetic tandem duplication of a BMC-H protein [201] and a BMC-T shell protein with inverted sidedness [202], resulting in relatively homogeneous protein shells.

Novel Enzyme Design and Targeting

Concomitant with the development of empty protein shells derived from MCP proteins, methods for targeting novel cargo to those shells were developed. A number of groups were able to target fluorescent proteins to empty MCP shells using native targeting sequences (such as the 18 N-terminal residues of PduP) or synthetically designed targeting sequences with specific motifs [78, 117, 118, 120, 122, 203–206]. In addition, native targeting sequences were used to direct multiple heterologous proteins to the Pdu shell, thereby constructing a proof-of-concept bioreactor for the production of ethanol [123]. Another attractive direction for the design of bespoke MCP shells is the sequestration of toxic products. Yung and colleagues were able to increase expression of lysis protein E from bacteriophage Φx174 by fusing it to an MCP targeting sequence and recombinantly co-expressing it with Pdu shell proteins [207]. In another example, an engineered MCP for the removal of phosphate contaminants from wastewater was developed by targeting polyphosphate kinase (PPK1) to an empty Pdu MCP through fusion with a PduP targeting sequence [203]. This allowed an 8-fold increase in cellular phosphate accumulation, apparently by blocking competing reactions that break down polyphosphate [199]. More recently, approaches to improve the targeting efficiency of cargo directed to MCP-based protein shells were pioneered by fusing shell and cargo proteins to non-native binding partners including scaffolding domains (SH3, PDZ and GBD), a split coiled-coil domain, or the spy-tag spy-catcher system [186, 204, 208]. Both proteins and small molecules have also been encapsulated within minimal shells derived from MCPs by *in vitro* loading during assembly on an oil-water interface [199]. Lastly, we mention that empty MCP shells and protein targeting systems have been engineered into industrially important organisms

including the thermophilic Bacilli and Corynebacteria [204, 206]. Thus, substantial progress has been made on targeting desired cargo to protein shells built from MCP proteins.

Current models for MCPs propose that optimal function requires a selectively permeable protein shell. Accordingly, work aimed at controlling shell permeability has begun. So far, this work has focused on modifying the pores present in shell proteins by site-directed mutagenesis and by constructing hybrid shells using BMC proteins derived from different MCPs [111, 163, 179, 181]. As mentioned above, there are many aspects of shell permeability that are poorly understood. Hence, further work will be needed before shells with desired permeability can be engineered.

Another notable biotechnology application is the use of MCPs to construct hybrid enzyme-inorganic catalysts [209]. In a recent study, gold nanoparticles were fabricated onto the surface of purified Pdu MCPs. The gold nanoparticle-MCPs retained the native diol dehydratase activity in the MCP interior and also possessed inorganic activity from the gold nanoparticles on the MCP exterior. This is a first step toward developing hybrid catalysts based on MCPs.

Current Challenges and Open Questions

Although many aspects of MCP structure, function, and physiology have been elucidated, open questions remain. Genetic characterization has revealed many MCP components and their general roles in product production, assembly, and bacterial growth. However, in many cases their particular mechanisms of action, as well as specific locations within (or in some cases, potentially outside) the microcompartments remain to be determined. Additionally, while crystal structures of individual MCP proteins have advanced the understanding of MCP composition, function, and assembly, how MCP parts work together, both structurally and enzymatically, to build and maintain a complete bioreactor has yet to be determined.

The pathways by which metabolosomes assemble remain only partly understood. Current findings suggest different assembly mechanisms between classes of carboxysomes [185, 210, 211], therefore it is possible that each metabolosome class possesses its own assembly framework. Relatedly, while many protein-protein interactions that govern MCP assembly have been determined, many more, particularly those that mediate assembly of the core and its interaction with the shell, are only beginning to be understood. Moreover, once an MCP is assembled, it is unclear how MCP structure enhances substrate processing. Despite an understanding of the mechanistic pathway taking place within the MCP, there are many unanswered questions about how MCP interiors are organized, and in turn, how these compartments interact with host cells.

A particularly intriguing question about MCPs is how their shells mediate the selective movement of small molecules. The size and chemical properties of the central pores of BMC-H proteins are thought to allow the selective diffusion of MCP substrates. However, the manner in which MCP products and enzymatic cofactors move across the shell has not been worked out. Dynamic gates in BMC-T proteins have been proposed but not demonstrated experimentally. Furthermore, many MCPs include only a single gated trimer, and how a single gate would mediate the movement of several different cofactors is unclear.

In addition, electron transfer through shell proteins with [Fe-S] clusters has been suggested but not experimentally demonstrated.

It is also of note that as large, complex organelles, MCPs are energetically costly to the cell. The stability and longevity of these compartments remain unclear, and these aspects in particular may have implications for inhibiting pathogenic and commensal bacteria to optimize health. Further, an understanding of MCP stability would allow improved engineering for designing compartments, allowing them to survive in harsh environments to sequester toxic species or dissociate predictably at the site of drug delivery.

The diversity of bacterial MCPs is another area where further study is likely to yield rewards. Many diverse MCPs found throughout the domains of bacteria have been studied very little or not at all. In some cases, MCP substrates are unknown and almost no work has been done on how MCPs fit into the broader metabolic schemes of their host organisms. Future work in these areas promises to uncover interesting biochemistry, advance bioengineering and biomedical applications, and broaden our understanding of bacterial physiology and pathogenesis. Furthermore, we expect that ongoing studies of these sophisticated organelles in the context of the *Salmonella* an *E. coli* hosts will drive advances in many of the areas mentioned above.

References

[1]. Chowdhury C, Sinha S, Chun S, Yeates TO, Bobik TA. Diverse bacterial microcompartment organelles. Microbiol Mol Biol Rev. 2014;78:438–68. [PubMed: 25184561]

[2]. Kerfeld CA, Aussignargues C, Zarzycki J, Cai F, Sutter M. Bacterial microcompartments. Nature Rev Microbio. 2018;16:277–90.

[3]. Rae BD, Long BM, Badger MR, Price GD. Functions, compositions, and evolution of the two types of carboxysomes: Polyhedral microcompartments that facilitate CO2 fixation in cyanobacteria and some proteobacteria. Microbiol Mol Biol Rev. 2013;77:357–79. [PubMed: 24006469]

[4]. Axen SD, Erbilgin O, Kerfeld CA. A taxonomy of bacterial microcompartment loci constructed by a novel scoring method. PLoS Comp Biol. 2014;10:e1003898.

[5]. Abdul-Rahman F, Petit E, Blanchard JL. The distribution of polyhedral bacterial microcompartments suggests frequent horizontal transfer and operon reassembly. J Phylo Evo Bio. 2013;01:1–7.

[6]. Jorda J, Lopez D, Wheatley NM, Yeates TO. Using comparative genomics to uncover new kinds of protein-based metabolic organelles in bacteria. Protein Sci. 2013;22:179–95. [PubMed: 23188745]

[7]. Zarzycki J, Erbilgin O, Kerfeld CA. Bioinformatic characterization of glycyl radical enzyme-associated bacterial microcompartments. Appl Environ Microbiol. 2015;81:8315–29. [PubMed: 26407889]

[8]. Bobik TA. Polyhedral organelles compartmenting bacterial metabolic processes. Appl Microbiol Biotechnol. 2006;70:517–25. [PubMed: 16525780]

[9]. Yeates TO, Jorda J, Bobik TA. The shells of BMC-type microcompartment organelles in bacteria. J Mol Microbiol Biotechnol. 2013;23:290–9. [PubMed: 23920492]

[10]. Roth J, Lawrence J, Bobik T. Cobalamin (coenzyme B12): Synthesis and biological significance. Annu Rev Microbiol. 1996;50:137–81. [PubMed: 8905078]

[11]. Garsin DA. Ethanolamine utilization in bacterial pathogens: Roles and regulation. Nature Rev Microbio. 2010;8:290–5.

[12]. Wang Z, Klipfell E, Bennett BJ, Koeth R, Levison BS, Dugar B, Feldstein AE, Britt EB, Fu X, Chung YM, Wu Y, Schauer P, Smith JD, Allayee H, Tang WHW, Didonato JA, Lusis AJ, Hazen

SL. Gut flora metabolism of phosphatidylcholine promotes cardiovascular disease. Nature. 2011;472:57–65. [PubMed: 21475195]

[13]. Bae S, Ulrich CM, Neuhouser ML, Malysheva O, Bailey LB, Xiao L, Brown EC, Cushing-Haugen KL, Zheng Y, Cheng TYD, Miller JW, Green R, Lane DS, Beresford SaA, Caudill MA. Plasma choline metabolites and colorectal cancer risk in the women's health initiative observational study. Cancer Res. 2014;74:7442–52. [PubMed: 25336191]

[14]. Frank S, Lawrence AD, Prentice MB, Warren MJ. Bacterial microcompartments moving into a synthetic biological world. J Biotechnol. 2013;163:273–9. [PubMed: 22982517]

[15]. Kim EY, Tullman-Ercek D. Engineering nanoscale protein compartments for synthetic organelles. Curr Opin Biotechnol. 2013;24:627–32. [PubMed: 23273660]

[16]. Plegaria JS, Kerfeld CA. Engineering nanoreactors using bacterial microcompartment architectures. Curr Opin Biotechnol. 2018;51:1–7. [PubMed: 29035760]

[17]. Tsai SJ, Yeates TO. Bacterial microcompartments: Insights into the structure, mechanism, and engineering applications. Prog Mol Biol Transl Sci. 2011;103:1–20. [PubMed: 21999993]

[18]. Drews G, Niklowitz W. Beiträge zur cytologie der blaualgen - II. Mittelung zentroplasma und granuläre einschlüsse von phormidium uncinatum. Arch Mikrobiol. 1956;24:147–62. [PubMed: 13327992]

[19]. Badger MR, Price GD. CO2 concentrating mechanisms in cyanobacteria: Molecular components, their diversity and evolution. J Exp Bot. 2003;54:609–22. [PubMed: 12554704]

[20]. Cannon GC, Heinhorst S, Bradburne CE, Shively JM. Carboxysome genomics: A status report. Funct Plant Biol. 2002;29:175–82. [PubMed: 32689464]

[21]. Shively JM, Ball F, Brown DH, Saunders RE. Functional organelles in prokaryotes: Polyhedral inclusions (carboxysomes) of Thiobacillus neapolitanus. Science. 1973;182:584–6. [PubMed: 4355679]

[22]. Bobik TA, Havemann GD, Busch RJ, Williams DS, Aldrich HC. The propanediol utilization (pdu) operon of Salmonella enterica serovar Typhimurium LT2 includes genes necessary for formation of polyhedral organelles involved in coenzyme B12-dependent 1,2-propanediol degradation. J Bacteriol. 1999;181:5967–75. [PubMed: 10498708]

[23]. Kofoid E, Rappleye C, Stojiljkovic I, Roth J. The 17-gene ethanolamine (eut) operon of Salmonella typhimurium encodes five homologues of carboxysome shell proteins. J Bacteriol. 1999;181:5317–29. [PubMed: 10464203]

[24]. Erbilgin O, Mcdonald KL, Kerfeld CA. Characterization of a planctomycetal organelle: A novel bacterial microcompartment for the aerobic degradation of plant saccharides. Appl Environ Microbiol. 2014;80:2193–205. [PubMed: 24487526]

[25]. Sriramulu DD, Liang M, Hernandez-Romero D, Raux-Deery E, Lünsdorf H, Parsons JB, Warren MJ, Prentice MB. Lactobacillus reuteri DSM 20016 produces cobalamin-dependent diol dehydratase in metabolosomes and metabolizes 1,2-propanediol by disproportionation. J Bacteriol. 2008;190:4559–67. [PubMed: 18469107]

[26]. Talarico TL, Axelsson LT, Novotny J, Fiuzat M, Dobrogosz WJ. Utilization of glycerol as a hydrogen acceptor by Lactobacillus reuteri: Purification of 1,3-propanediol:NAD+ oxidoreductase. Appl Environ Microbiol. 1990;56:943–8. [PubMed: 16348177]

[27]. Petit E, Latouf WG, Coppi MV, Warnick TA, Currie D, Romashko I, Deshpande S, Haas K, Alvelo-Maurosa JG, Wardman C, Schnell DJ, Leschine SB, Blanchard JL. Involvement of a bacterial microcompartment in the metabolism of fucose and rhamnose by Clostridium phytofermentans. PLoS ONE. 2013;8.

[28]. Jameson E, Fu T, Brown IR, Paszkiewicz K, Purdy KJ, Frank S, Chen Y. Anaerobic choline metabolism in microcompartments promotes growth and swarming of Proteus mirabilis. Environ Microbiol. 2016;18:2886–98. [PubMed: 26404097]

[29]. Lundin AP, Stewart KL, Stewart AM, Herring TI, Chowdhury C, Bobik TA. Genetic characterization of a glycyl radical microcompartment used for 1,2-Propanediol fermentation by uropathogenic Escherichia coli CFT073 J Bacteriol. 2020;202.

[30]. Herring TI, Harris TN, Chowdhury C, Mohanty SK, Bobik TA. A bacterial microcompartment is used for choline fermentation by Escherichia coli 536. J Bacteriol. 2018;200:1–13.

[31]. Sampson EM, Bobik TA. Microcompartments for B12-dependent 1,2-propanediol degradation provide protection from DNA and cellular damage by a reactive metabolic intermediate. J Bacteriol. 2008;190:2966–71. [PubMed: 18296526]

[32]. Rondon MR, Horswill AR, Escalante-Semerena JC. DNA polymerase I function is required for the utilization of ethanolamine, 1,2-propanediol, and propionate by Salmonella typhimurium LT2. J Bacteriol. 1995;177:7119–24. [PubMed: 8522518]

[33]. Penrod JT, Roth JR. Conserving a volatile metabolite: A role for carboxysome-like organelles in Salmonella enterica. J Bacteriol. 2006;188:2865–74. [PubMed: 16585748]

[34]. Brinsmade SR, Paldon T, Escalante-Semerena JC. Minimal functions and physiological conditions required for growth of Salmonella enterica on ethanolamine in the absence of the metabolosome. J Bacteriol. 2005;187:8039–46. [PubMed: 16291677]

[35]. Jakobson CM, Tullman-Ercek D, Slininger MF, Mangan NM. A systems-level model reveals that 1,2-Propanediol utilization microcompartments enhance pathway flux through intermediate sequestration. PLoS Comp Biol. 2017;13:1–24.

[36]. Kendall MM, Gruber CC, Parker CT, Sperandio V. Ethanolamine controls expression of genes encoding components involved in interkingdom signaling and virulence in enterohemorrhagic Escherichia coli O157:H7. mBio. 2012;3:1–10.

[37]. Maadani A, Fox KA, Mylonakis E, Garsin DA. Enterococcus faecalis mutations affecting virulence in the Caenorhabditis elegans model host. Infect Immun. 2007;75:2634–7. [PubMed: 17307944]

[38]. Ormsby MJ, Logan M, Johnson SA, Mcintosh A, Fallata G, Papadopoulou R, Papachristou E, Hold GL, Hansen R, Ijaz UZ, Russell RK, Gerasimidis K, Wall DM. Inflammation associated ethanolamine facilitates infection by Crohn's disease-linked adherent-invasive Escherichia coli. EBioMed. 2019;43:325–32.

[39]. Dadswell K, Creagh S, Mccullagh E, Liang M, Brown IR, Warren MJ, Mcnally A, Macsharry J, Prentice MB. Bacterial microcompartment-mediated ethanolamine metabolism in Escherichia coli urinary tract infection. Infect Immun. 2019;87:e00211–e9. [PubMed: 31138611]

[40]. Klumpp J, Fuchs TM. Identification of novel genes in genomic islands that contribute to Salmonella typhimurium replication in macrophages. Microbiology. 2007;153:1207–20. [PubMed: 17379730]

[41]. Harvey PC, Watson M, Hulme S, Jones MA, Lovell M, Berchieri J, Young J, Bumstead N, Barrow P. Salmonella enterica serovar typhimurium colonizing the lumen of the chicken intestine grows slowly and upregulates a unique set of virulence and metabolism genes. Infect Immun. 2011;79:4105–21. [PubMed: 21768276]

[42]. Thiennimitr P, Winter SE, Winter MG, Xavier MN, Tolstikov V, Huseby DL, Sterzenbach T, Tsolis RM, Roth JR, Bäumler AJ. Intestinal inflammation allows Salmonella to use ethanolamine to compete with the microbiota. Proc Natl Acad Sci. 2011;108:17480–5. [PubMed: 21969563]

[43]. Winter SE, Thiennimitr P, Winter MG, Butler BP, Huseby DL, Crawford RW, Russell JM, Bevins CL, Adams LG, Tsolis RM, Roth JR, Bäumler AJ. Gut inflammation provides a respiratory electron acceptor for Salmonella. Nature. 2010;467:426–9. [PubMed: 20864996]

[44]. Jakobson CM, Tullman-Ercek D. Dumpster diving in the gut: Bacterial microcompartments as part of a host-associated lifestyle. PLoS Path. 2016;12:10–4.

[45]. Joseph B, Przybilla K, Stühler C, Schauer K, Slaghuis J, Fuchs TM, Goebel W. Identification of Listeria monocytogenes genes contributing to intracellular replication by expression profiling and mutant screening. J Bacteriol. 2006;188:556–68. [PubMed: 16385046]

[46]. Faber F, Thiennimitr P, Spiga L, Byndloss MX, Litvak Y, Lawhon S, Andrews-Polymenis HL, Winter SE, Bäumler AJ. Respiration of microbiota-derived 1,2-propanediol drives Salmonella expansion during colitis. PLoS Path. 2017;13.

[47]. Romano KA, Martinez-Del Campo A, Kasahara K, Chittim CL, Vivas EI, Amador-Noguez D, Balskus EP, Rey FE. Metabolic, epigenetic, and transgenerational effects of gut bacterial choline consumption. Cell Host Micro. 2017;22:279–90.e7.

[48]. Tang WHW, Kitai T, Hazen SL. Gut microbiota in cardiovascular health and disease. Circul Res. 2017;120:1183–96.

[49]. Chen YM, Liu Y, Zhou RF, Chen XL, Wang C, Tan XY, Wang LJ, Zheng RD, Zhang HW, Ling WH, Zhu HL. Associations of gut-flora-dependent metabolite trimethylamine-N-oxide, betaine and choline with non-alcoholic fatty liver disease in adults. Sci Rep. 2016;6:1–9. [PubMed: 28442746]

[50]. Jie Z, Xia H, Zhong SL, Feng Q, Li S, Liang S, Zhong H, Liu Z, Gao Y, Zhao H, Zhang D, Su Z, Fang Z, Lan Z, Li J, Xiao L, Li J, Li R, Li X, Li F, Ren H, Huang Y, Peng Y, Li G, Wen B, Dong B, Chen JY, Geng QS, Zhang ZW, Yang H, Wang J, Wang J, Zhang X, Madsen L, Brix S, Ning G, Xu X, Liu X, Hou Y, Jia H, He K, Kristiansen K. The gut microbiome in atherosclerotic cardiovascular disease. Nature Coms. 2017;8:845.

[51]. Trøseid M, Ueland T, Hov JR, Svardal A, Gregersen I, Dahl CP, Aakhus S, Gude E, Bjørndal B, Halvorsen B, Karlsen TH, Aukrust P, Gullestad L, Berge RK, Yndestad A. Microbiota-dependent metabolite trimethylamine-N-oxide is associated with disease severity and survival of patients with chronic heart failure. J Intern Med. 2015;277:717–26. [PubMed: 25382824]

[52]. Moraes C, Fouque D, Amaral ACF, Mafra D. Trimethylamine N-oxide From gut microbiota in chronic kidney disease patients: Focus on diet. J Ren Nutr2015 p. 459–65. [PubMed: 26235933]

[53]. Xu KY, Xia GH, Lu JQ, Chen MX, Zhen X, Wang S, You C, Nie J, Zhou HW, Yin J. Impaired renal function and dysbiosis of gut microbiota contribute to increased trimethylamine-N-oxide in chronic kidney disease patients. Sci Rep. 2017;7. [PubMed: 28127057]

[54]. Tang WHW, Wang Z, Li XS, Fan Y, Li DS, Wu Y, Hazen SL. Increased trimethylamine N-oxide portends high mortality risk independent of glycemic control in patients with type 2 diabetes mellitus. Clin Chem. 2017;63:297–306. [PubMed: 27864387]

[55]. Dambrova M, Latkovskis G, Kuka J, Strele I, Konrade I, Grinberga S, Hartmane D, Pugovics O, Erglis A, Liepinsh E. Diabetes is associated with higher trimethylamine N-oxide plasma levels. Exp Clin Endocrinol Diabetes. 2016;124:251–6. [PubMed: 27123785]

[56]. Obradors N, Badia J, Baldoma L, Aguilar J. Anaerobic metaoblism of the L-rhamnose fermentation product 1,2-propanediol in Salmonella typhimurium. J Bacteriol. 1988;170:2159–62. [PubMed: 3283105]

[57]. Lawrence JG, Roth JR. Evolution of coenzyme B12 synthesis among enteric bacteria: Evidence for loss and reacquisition of a multigene complex. Genetics. 1996;142:11–24. [PubMed: 8770581]

[58]. Kaval KG, Gebbie M, Goodson JR, Cruz MR, Winkler WC, Garsin DA. Ethanolamine utilization and bacterial microcompartment formation are subject to carbon catabolite repression. J Bacteriol. 2019;209:1–13.

[59]. Martínez-Del Campo A, Bodea S, Hamer HA, Marks JA, Haiser HJ, Turnbaugh PJ, Balskusa EP. Characterization and detection of a widely distributed gene cluster that predicts anaerobic choline utilization by human gut bacteria. mBio. 2015;6:1–12.

[60]. Ochman H, Selander RK. Standard reference strains of Escherichia coli from natural populations. J Bacteriol. 1984;157:690–3. [PubMed: 6363394]

[61]. Zarzycki J, Sutter M, Cortina NS, Erb TJ, Kerfeld CA. In vitro characterization and concerted function of three core enzymes of a glycyl radical enzyme-associated bacterial microcompartment. Sci Rep. 2017;7:1–12. [PubMed: 28127051]

[62]. Jeter RM. Cobalamin-dependent 1,2-propanediol utilization by Salmonella typhimurium. J Gen Microbiol. 1990;136:887–96. [PubMed: 2166132]

[63]. Price-Carter M, Tingey J, Bobik TA, Roth JR. The alternative electron acceptor tetrathionate supports B12-dependent anaerobic growth of Salmonella enterica serovar typhimurium on ethanolamine or 1,2-propanediol. J Bacteriol. 2001;183:2463–75. [PubMed: 11274105]

[64]. Bobik TA, Xu Y, Jeter RM, Otto KE, Roth JR. Propanediol utilization genes (pdu) of Salmonella typhimurium: Three genes for the propanediol dehydratase. J Bacteriol. 1997;179:6633–9. [PubMed: 9352910]

[65]. Abeles RH, Lee HA. An intramolecular oxidation-reduction requiring a cobamide coenzyme. J Biol Chem. 1961;236:2347–50. [PubMed: 13680987]

[66]. Cheng S, Fan C, Sinha S, Bobik TA. The PduQ enzyme is an alcohol dehydrogenase used to recycle NAD+ internally within the Pdu microcompartment of Salmonella enterica. PLoS ONE. 2012;7:e47144. [PubMed: 23077559]

[67]. Leal NA, Havemann GD, Bobik TA. PduP is a coenzyme-a-acylating propionaldehyde dehydrogenase associated with the polyhedral bodies involved in B12-dependent 1,2-propanediol degradation by Salmonella enterica serovar Typhimurium LT2. Arch Microbiol. 2003;180:353–61. [PubMed: 14504694]

[68]. Liu Y, Leal NA, Sampson EM, Johnson CLV, Havemann GD, Bobik TA. PduL is an evolutionarily distinct phosphotransacylase involved in B12-dependent 1,2-propanediol degradation by Salmonella enterica serovar typhimurium LT2. J Bacteriol. 2007;189:1589–96. [PubMed: 17158662]

[69]. Palacios S, Starai VJ, Escalante-Semerena JC. Propionyl coenzyme A is a common intermediate in the 1,2-propanediol and propionate catabolic pathways needed for expression of the prpBCDE operon during growth of Salmonella enterica on 1,2-propanediol. J Bacteriol. 2003;185:2802–10. [PubMed: 12700259]

[70]. Horswill AR, Escalante-Semerena JC. Salmonella typhimurium LT2 catabolizes propionate via the 2-methylcitric acid cycle. J Bacteriol. 1999;181:5615–23. [PubMed: 10482501]

[71]. Cheng S, Bobik TA. Characterization of the PduS cobalamin reductase of Salmonella enterica and its role in the Pdu microcompartment. J Bacteriol. 2010;192:5071–80. [PubMed: 20656910]

[72]. Johnson CLV, Pechonick E, Park SD, Havemann GD, Leal NA, Bobik TA. Functional genomic, biochemical, and genetic characterization of the Salmonella pduO gene, an ATP:cob(I)alamin adenosyltransferase gene. J Bacteriol. 2001;183:1577–84. [PubMed: 11160088]

[73]. Walter D, Ailion M, Roth J. Genetic characterization of the pdu operon: Use of 1,2-propanediol in Salmonella typhimurium. J Bacteriol. 1997;179:1013–22. [PubMed: 9023178]

[74]. Sinha S, Cheng S, Fan C, Bobik TA. The PduM protein is a structural component of the microcompartments involved in coenzyme B12-dependent 1,2-propanediol degradation by Salmonella enterica. J Bacteriol. 2012;194:1912–8. [PubMed: 22343294]

[75]. Liu Y, Jorda J, Yeates TO, Bobik TA. The PduL phosphotransacylase is used to recycle coenzyme A within the Pdu microcompartment. J Bacteriol. 2015;197:2392–9. [PubMed: 25962918]

[76]. Cheng S, Sinha S, Fan C, Liu Y, Bobik TA. Genetic analysis of the protein shell of the microcompartments involved in coenzyme B12-dependent 1,2-propanediol degradation by Salmonella. J Bacteriol. 2011;193:1385–92. [PubMed: 21239588]

[77]. Havemann GD, Sampson EM, Bobik TA. PduA is a shell protein of polyhedral organelles involved in coenzyme B12-dependent degradation of 1,2-propanediol in Salmonella enterica serovar typhimurium LT2. J Bacteriol. 2002;184:1253–61. [PubMed: 11844753]

[78]. Parsons JB, Frank S, Bhella D, Liang M, Prentice MB, Mulvihill DP, Warren MJ. Synthesis of empty bacterial microcompartments, directed organelle protein incorporation, and evidence of filament-associated organelle movement. Mol Cell. 2010;38:305–15. [PubMed: 20417607]

[79]. Fan C, Fromm HJ, Bobik TA. Kinetic and functional analysis of L-threonine kinase, the PduX enzyme of Salmonella enterica. J Biol Chem. 2009;284:20240–8. [PubMed: 19509296]

[80]. Fan C, Bobik TA. The PduX enzyme of Salmonella enterica is an L-threonine kinase used for coenzyme B12 synthesis. J Biol Chem. 2008;283:11322–9. [PubMed: 18308727]

[81]. Rondon MR, Escalante-Semerena JC. In vitro analysis of the interactions between the PocR regulatory protein and the promoter region of the cobalamin biosynthetic (cob) operon of Salmonella typhimurium LT2. J Bacteriol. 1996;178:2196–203. [PubMed: 8636018]

[82]. Bobik TA, Ailion M, Roth JR. A single regulatory gene integrates control of vitamin B12 synthesis and propanediol degradation. J Bacteriol. 1992;174:2253–66. [PubMed: 1312999]

[83]. Ailion M, Bobik TA, Roth JR. Two global regulatory systems (Crp and Arc) control the cobalamin/propanediol regulon of Salmonella typhimurium. J Bacteriol. 1993;175:7200–8. [PubMed: 8226666]

[84]. Andersson DI. Involvement of the Arc system in redox regulation of the cob operon in Salmonella typhimurium. Mol Microbiol. 1992;6:1491–4. [PubMed: 1625578]

[85]. Lawhon SD, Frye JG, Suyemoto M, Porwollik S, Mcclelland M, Altier C. Global regulation by CsrA in Salmonella typhimurium. Mol Microbiol. 2003;48:1633–45. [PubMed: 12791144]

[86]. Wang Z, Sun J, Tian M, Xu Z, Liu Y, Fu J, Yan A, Liu X. Proteomic analysis of FNR-regulated anaerobiosis in Salmonella typhimurium. J Am Soc Mass Spectrom. 2019;30:1001–12. [PubMed: 30903387]

[87]. Roof DM, Roth JR. Ethanolamine utilization in Salmonella typhimurium. J Bacteriol. 1988;170:3855–63. [PubMed: 3045078]

[88]. Roof DM, Roth JR. Functions required for vitamin B12-dependent ethanolamine utilization in Salmonella typhimurium. J Bacteriol. 1989;171:3316–23. [PubMed: 2656649]

[89]. Jeter RM, Olivera BM, Roth JR. Salmonella typhimurium synthesizes cobalamin (vitamin B12) de novo under anaerobic growth conditions. J Bacteriol. 1984;159:206–13. [PubMed: 6376471]

[90]. Bobik TA, Lehman BP, Yeates TO. Bacterial microcompartments: Widespread prokaryotic organelles for isolation and optimization of metabolic pathways. Mol Microbiol. 2015;98:193–207. [PubMed: 26148529]

[91]. Shibata N, Tamagaki H, Hieda N, Akita K, Komori H, Shomura Y, Terawaki SI, Mori K, Yasuoka N, Higuchi Y, Toraya T. Crystal structures of ethanolamine ammonia-lyase complexed with coenzyme B12 analogs and substrates. J Biol Chem. 2010;285:26484–93. [PubMed: 20519496]

[92]. Zhu H, Gonzalez R, Bobik TA. Coproduction of acetaldehyde and hydrogen during glucose fermentation by Escherichia coli. Appl Environ Microbiol. 2011;77:6441–50. [PubMed: 21803884]

[93]. Huseby DL, Roth JR. Evidence that a metabolic microcompartment contains and recycles private cofactor pools. J Bacteriol. 2013;195:2864–79. [PubMed: 23585538]

[94]. Buan NR, Suh SJ, Escalante-Semerena JC. The eutT gene of Salmonella enterica encodes an oxygen-labile, metal-containing ATP:Corrinoid adenosyltransferase enzyme J Bacteriol. 2004;186:7826.

[95]. Sheppard DE, Penrod JT, Bobik T, Kofoid E, Roth JR. Evidence that a B12-adenosyl transferase is encoded within the ethanolamine operon of Salmonella enterica. J Bacteriol. 2004;186:7635–44. [PubMed: 15516577]

[96]. Mori K, Bando R, Hieda N, Toraya T. Identification of a reactivating factor for adenosylcobalamin-dependent ethanolamine ammonia lyase. J Bacteriol. 2004;186:6845–54. [PubMed: 15466038]

[97]. Moore TC, Escalante-Semerena JC. The EutQ and EutP proteins are novel acetate kinases involved in ethanolamine catabolism: Physiological implications for the function of the ethanolamine metabolosome in Salmonella enterica. Mol Microbiol. 2016;99:497–511. [PubMed: 26448059]

[98]. Stojiljkovic I, Baumler AJ, Heffron F. Ethanolamine utilization in Salmonella typhimurium: Nucleotide sequence, protein expression, and mutational analysis of the cchA cchB eutE eutJ eutG eutH gene cluster. J Bacteriol. 1995;177:1357–66. [PubMed: 7868611]

[99]. Bandarian V, Poyner RR, Reed GH. Hydrogen atom exchange between 5'-deoxyadenosine and hydroxyethylhydrazine during the single turnover inactivation of ethanolamine ammonia-lyase. Biochemistry. 1999;38:12403–7. [PubMed: 10493808]

[100]. Bandarian V, Reed GH. Hydrazine cation radical in the active site of ethanolamine ammonia-lyase: Mechanism-based inactivation by hydroxyethylhydrazine. Biochemistry. 1999;38:12394–402. [PubMed: 10493807]

[101]. Bologna FP, Campos-Bermudez VA, Saavedra DD, Andreo CS, Drincovich MF. Characterization of Escherichia coli EutD: A phosphotransacetylase of the ethanolamine operon. J Microbio. 2010;48:629–36.

[102]. Buan NR, Escalante-Semerena JC. Purification and initial biochemical characterization of ATP:Cob(I)alamin adenosyltransferase (EutT) enzyme of Salmonella enterica. J Biol Chem. 2006;281:16971–7. [PubMed: 16636051]

[103]. Held M, Kolb A, Perdue S, Hsu SY, Bloch SE, Quin MB, Schmidt-Dannert C. Engineering formation of multiple recombinant Eut protein nanocompartments in E. coli. Sci Rep. 2016;6:24359. [PubMed: 27063436]

[104]. Penrod JT, Mace CC, Roth JR. A pH-sensitive function and phenotype: Evidence that EutH facilitates diffusion of uncharged ethanolamine in Salmonella enterica. J Bacteriol. 2004;186:6885–90. [PubMed: 15466042]

[105]. Roof DM, Roth JR. Autogenous regulation of ethanolamine utilization by a transcriptional activator of the eut operon in Salmonella typhimurium. J Bacteriol. 1992;174:6634–43. [PubMed: 1328159]

[106]. Sheppard DE, Roth JR. A rationale for autoinduction of a transcriptional activator: Ethanolamine ammonia-lyase (EutBC) and the operon activator (EutR) compete for adenosyl-cobalamin in Salmonella typhimurium. J Bacteriol. 1994;176:1287–96. [PubMed: 8113167]

[107]. Shimada T, Fujita N, Yamamoto K, Ishihama A. Novel roles of camp receptor protein (CRP) in regulation of transport and metabolism of carbon sources. PLoS ONE. 2011;6:e20081. [PubMed: 21673794]

[108]. Busby S, Ebright RH. Transcription activation by catabolite activator protein (CAP). J Mol Biol. 1999;293:199–213. [PubMed: 10550204]

[109]. Sturms R, Streauslin NA, Cheng S, Bobik TA. In Salmonella enterica, ethanolamine utilization is repressed by 1,2-propanediol to prevent detrimental mixing of components of two different bacterial microcompartments. J Bacteriol. 2015;197:2412–21. [PubMed: 25962913]

[110]. Jakobson CM, Kim EY, Slininger MF, Chien A, Tullman-Ercek D. Localization of proteins to the 1,2-propanediol utilization microcompartment by non-native signal sequences is mediated by a common hydrophobic motif. J Biol Chem. 2015;290:24519–33. [PubMed: 26283792]

[111]. Slininger Lee MF, Jakobson CM, Tullman-Ercek D. Evidence for improved encapsulated pathway behavior in a bacterial microcompartment through shell protein engineering. ACS Synth Bio. 2017;6:1880–91. [PubMed: 28585808]

[112]. Craciun S, Balskus EP. Microbial conversion of choline to trimethylamine requires a glycyl radical enzyme. Proc Natl Acad Sci. 2012;109:21307–12. [PubMed: 23151509]

[113]. Kalnins G, Kuka J, Grinberga S, Makrecka-Kuka M, Liepinsh E, Dambrova M, Tars K. Structure and function of CutC choline lyase from human microbiota bacterium Klebsiella pneumoniae. J Biol Chem. 2015;290:21732–40. [PubMed: 26187464]

[114]. Dobrindt U, Blum-Oehler G, Nagy G, Schneider G, Johann A, Gottschalk G, Hacker J. Genetic structure and distribution of four pathogenicity islands (PAI I536 to PAI IV536) of uropathogenic Escherichia coli strain 536. Infect Immun. 2002;70:6365–72. [PubMed: 12379716]

[115]. Schindel HS, Karty JA, Mckinlay JB, Bauer CE. Characterization of a glycyl radical enzyme bacterial microcompartment pathway in Rhodobacter capsulatus. J Bacteriol. 2019;201:e00343–18. [PubMed: 30510145]

[116]. Fan C, Cheng S, Liu Y, Escobar CM, Crowley CS, Jefferson RE, Yeates TO, Bobik TA. Short N-terminal sequences package proteins into bacterial microcompartments. Proc Natl Acad Sci. 2010;107:7509–14. [PubMed: 20308536]

[117]. Fan C, Bobik TA. The N-terminal region of the medium subunit (PduD) packages adenosylcobalamin-dependent diol dehydratase (PduCDE) into the Pdu microcompartment. J Bacteriol. 2011;193:5623–8. [PubMed: 21821773]

[118]. Choudhary S, Quin MB, Sanders MA, Johnson ET, Schmidt-Dannert C. Engineered protein nanocompartments for targeted enzyme localization. PLoS ONE. 2012;7:e33342. [PubMed: 22428024]

[119]. Fan C, Cheng S, Sinha S, Bobik TA. Interactions between the termini of lumen enzymes and shell proteins mediate enzyme encapsulation into bacterial microcompartments. Proc Natl Acad Sci. 2012;109:14995–5000. [PubMed: 22927404]

[120]. Quin MB, Perdue SA, Hsu SY, Schmidt-Dannert C. Encapsulation of multiple cargo proteins within recombinant Eut nanocompartments. Appl Microbiol Biotechnol. 2016;100:9187–200. [PubMed: 27450681]

[121]. Kinney JN, Salmeen A, Cai F, Kerfeld CA. Elucidating essential role of conserved carboxysomal protein CcmN reveals common feature of bacterial microcompartment assembly. J Biol Chem. 2012;287:17729–36. [PubMed: 22461622]

[122]. Kim EY, Tullman-Ercek D. A rapid flow cytometry assay for the relative quantification of protein encapsulation into bacterial microcompartments. Biotechnol J. 2014;9:348–54. [PubMed: 24323373]

[123]. Lawrence AD, Frank S, Newnham S, Lee MJ, Brown IR, Xue WF, Rowe ML, Mulvihill DP, Prentice MB, Howard MJ, Warren MJ. Solution structure of a bacterial microcompartment targeting peptide and its application in the construction of an ethanol bioreactor. ACS Synth Bio. 2014;3:454–65. [PubMed: 24933391]

[124]. Yang M, Simpson DM, Wenner N, Brownridge P, Harman VM, Hinton JCD, Beynon RJ, Liu L-N. Decoding the stoichiometric composition and organisation of bacterial metabolosomes. Nature Coms. 2020:1–11.

[125]. Toraya T Cobalamin-dependent dehydratases and a deaminase: Radical catalysis and reactivating chaperones. Arch Biochem Biophys. 2014;544:40–57. [PubMed: 24269950]

[126]. Akita K, Hieda N, Baba N, Kawaguchi S, Sakamoto H, Nakanishi Y, Yamanishi M, Mori K, Toraya T. Purification and some properties of wild-type and N-terminal-truncated ethanolamine ammonia-lyase of Escherichia coli. J Biochem. 2010;147:83–93. [PubMed: 19762342]

[127]. Toraya T Radical catalysis in coenzyme B12-dependent isomerization (eliminating) reactions. Chem Rev. 2003;103:2095–127. [PubMed: 12797825]

[128]. Johnson CLV, Buszko ML, Bobik TA. Purification and initial characterization of the Salmonella enterica PduO ATP:Cob(I)alamin adenosyltransferase. J Bacteriol. 2004;186:7881–7. [PubMed: 15547259]

[129]. Wagner OW, Lee HA, Frey PA, Abeles RH. Studies on the mechanism of action of cobamide coenzymes: Chemical properties of the enzyme-coenzyme complex. J Biol Chem. 1966;241:1751–62. [PubMed: 5945850]

[130]. Bachovchin WW, Eagar RG, Moore KW, Richards JH. Mechanism of action of adenosylcobalamin: Glycerol and other substrate analogues as substrates and inactivators for propanediol dehydratase—kinetics, stereospecificity, and mechanism. Biochemistry. 1977;16:1082–92. [PubMed: 321014]

[131]. Yamanishi M, Kinoshita K, Fukuoka M, Saito T, Tanokuchi A, Ikeda Y, Obayashi H, Mori K, Shibata N, Tobimatsu T, Toraya T. Redesign of coenzyme B12 dependent diol dehydratase to be resistant to the mechanism-based inactivation by glycerol and act on longer chain 1,2-diols. FEBS J. 2012;279:793–804. [PubMed: 22221669]

[132]. Daniel R, Bobik TA, Gottschalk G. Biochemistry of coenzyme B12 -dependent glycerol and diol dehydratases and organization of the encoding genes FEMS Microbiol Rev. 1998;22:553–66. [PubMed: 9990728]

[133]. Toraya T Radical catalysis of B12 enzymes: Structure, mechanism, inactivation, and reactivation of diol and glycerol dehydratases. Cell Mol Life Sci. 2000;57:106–27. [PubMed: 10949584]

[134]. Mori K, Hosokawa Y, Yoshinaga T, Toraya T. Diol dehydratase-reactivating factor is a reactivase: Evidence for multiple turnovers and subunit swapping with diol dehydratase. FEBS J. 2010;277:4931–43. [PubMed: 21040475]

[135]. Mori K, Obayashi K, Hosokawa Y, Yamamoto A, Yano M, Yoshinaga T, Toraya T. Essential roles of nucleotide-switch and metal-coordinating residues for chaperone function of diol dehydratase-reactivase. Biochemistry. 2013;52:8677–86. [PubMed: 24229359]

[136]. Sampson EM, Johnson CLV, Bobik TA. Biochemical evidence that the pduS gene encodes a bifunctional cobalamin reductase. Microbiology. 2005;151:1169–77. [PubMed: 15817784]

[137]. Fonseca MV, Escalante-Semerena JC. An in vitro reducing system for the enzymic conversion of cobalamin to adenosylcobalamin. J Biol Chem. 2001;276:32101–8. [PubMed: 11408479]

[138]. Fonseca MV, Escalante-Semerena JC. Reduction of cob(III)alamin to cob(II)alamin in Salmonella enterica serovar typhimurium LT2. J Bacteriol. 2000;182:4304–9. [PubMed: 10894741]

[139]. Bovell AM, Warncke K. The structural model of salmonella typhimurium ethanolamine ammonia-lyase directs a rational approach to the assembly of the functional [(EutB-EutC)2]3 oligomer from isolated subunits. Biochemistry. 2013;52:1419–28. [PubMed: 23374068]

[140]. Shibata N, Masuda J, Tobimatsu T, Toraya T, Suto K, Morimoto Y, Yasuoka N. A new mode of B12 binding and the direct participation of a potassium ion in enzyme catalysis: X-ray structure of diol dehydratase. Structure. 1999;7:997–1008. [PubMed: 10467140]

[141]. Havemann GD, Bobik TA. Protein content of polyhedral organelles involved in coenzyme B12-dependent degradation of 1,2-propanediol in Salmonella enterica serovar typhimurium LT2. J Bacteriol. 2003;185:5086–95. [PubMed: 12923081]

[142]. Frey PA. Radical mechanisms of enzymatic catalysis. Annu Rev Biochem. 2001;70:121–48. [PubMed: 11395404]

[143]. Backman LRF, Funk MA, Dawson CD, Drennan CL. New tricks for the glycyl radical enzyme family. Crit Rev Biochem Mol Biol. 2017;52:674–95. [PubMed: 28901199]

[144]. Shisler KA, Broderick JB. Glycyl radical activating enzymes: Structure, mechanism, and substrate interactions. Arch Biochem Biophys. 2014;546:64–71. [PubMed: 24486374]

[145]. Bowman SEJ, Backman LRF, Bjork RE, Andorfer MC, Yori S, Caruso A, Stultz CM, Drennan CL. Solution structure and biochemical characterization of a spare part protein that restores activity to an oxygen-damaged glycyl radical enzyme. J Biol Inorg Chem. 2019;24:817–29. [PubMed: 31250200]

[146]. Bodea S, Balskus EP. Purification and characterization of the choline trimethylamine-lyase (CutC)-activating protein CutD. Methods Enzymol. 2018;606:73–94. [PubMed: 30097105]

[147]. Kalnins G, Cesle E-E, Jansons J, Liepins J, Filimonenko A, Tars K. Encapsulation mechanisms and structural studies of GRM2 bacterial microcompartment particles. Nature Coms. 2020;11:388.

[148]. Starai VJ, Garrity J, Escalante-Semerena JC. Acetate excretion during growth of Salmonella enterica on ethanolamine requires phosphotransacetylase (EutD) activity, and acetate recapture requires acetyl-CoA synthetase (Acs) and phosphotransacetylase (Pta) activities. Microbiology. 2005;151:3793–801. [PubMed: 16272400]

[149]. Erbilgin O, Sutter M, Kerfeld CA. The structural basis of coenzyme A recycling in a bacterial organelle. PLoS Biol. 2016;14:e1002399. [PubMed: 26959993]

[150]. Yeates TO, Thompson MC, Bobik TA. The protein shells of bacterial microcompartment organelles. Curr Opin Struct Biol. 2011;21:223–31. [PubMed: 21315581]

[151]. Tanaka S, Kerfeld CA, Sawaya MR, Cai F, Heinhorst S, Cannon GC, Yeates TO. Atomic-level models of the bacterial carboxysome shell. Science. 2008;319:1083–6. [PubMed: 18292340]

[152]. Sinha S, Cheng S, Sung YW, Mcnamara DE, Sawaya MR, Yeates TO, Bobik TA. Alanine scanning mutagenesis identifies an asparagine-arginine-lysine triad essential to assembly of the shell of the Pdu microcompartment. J Mol Biol. 2014;426:2328–45. [PubMed: 24747050]

[153]. Takenoya M, Nikolakakis K, Sagermann M. Crystallographic insights into the pore structures and mechanisms of the EutL and EutM shell proteins of the ethanolamine-utilizing microcompartment of Escherichia coli. J Bacteriol. 2010;192:6056–63. [PubMed: 20851901]

[154]. Crowley CS, Sawaya MR, Bobik TA, Yeates TO. Structure of the PduU shell protein from the Pdu microcompartment of Salmonella. Structure. 2008;16:1324–32. [PubMed: 18786396]

[155]. Crowley CS, Cascio D, Sawaya MR, Kopstein JS, Bobik TA, Yeates TO. Structural insight into the mechanisms of transport across the Salmonella enterica Pdu microcompartment shell. J Biol Chem. 2010;285:37838–46. [PubMed: 20870711]

[156]. Pang A, Warren MJ, Pickersgill RW. Structure of PduT, a trimeric bacterial microcompartment protein with a 4Fe-4S cluster binding site. Acta Crystallogr Sect D Biol Crystallogr. 2011;67:91–6. [PubMed: 21245529]

[157]. Thompson MC, Wheatley NM, Jorda J, Sawaya MR, Gidaniyan SD, Ahmed H, Yang Z, Mccarty KN, Whitelegge JP, Yeates TO. Identification of a unique Fe-S cluster binding site in a glycyl-radical type microcompartment shell protein. J Mol Biol. 2014;426:3287–304. [PubMed: 25102080]

[158]. Wheatley NM, Gidaniyan SD, Liu Y, Cascio D, Yeates TO. Bacterial microcompartment shells of diverse functional types possess pentameric vertex proteins. Protein Sci. 2013;22:660–5. [PubMed: 23456886]

[159]. Tanaka S, Sawaya MR, Yeates TO. Structure and mechanisms of a protein-based organelle in Escherichia coli. Science. 2010;327:81–4. [PubMed: 20044574]

[160]. Sagermann M, Ohtaki A, Nikolakakis K. Crystal structure of the EutL shell protein of the ethanolamine ammonia lyase microcompartment. Proc Natl Acad Sci. 2009;106:8883–7. [PubMed: 19451619]

[161]. Pang A, Liang M, Prentice MB, Pickersgill RW. Substrate channels revealed in the trimeric Lactobacillus reuteri bacterial microcompartment shell protein PduB. Acta Crystallogr Sect D Biol Crystallogr. 2012;68:1642–52. [PubMed: 23151629]

[162]. Chowdhury C, Chun S, Sawaya MR, Yeates TO, Bobik TA. The function of the PduJ microcompartment shell protein is determined by the genomic position of its encoding gene. Mol Microbiol. 2016;101:770–83. [PubMed: 27561553]

[163]. Chowdhury C, Chun S, Pang A, Sawaya MR, Sinha S, Yeates TO, Bobik TA. Selective molecular transport through the protein shell of a bacterial microcompartment organelle. Proc Natl Acad Sci. 2015;112:2990–5. [PubMed: 25713376]

[164]. Thompson MC, Cascio D, Leibly DJ, Yeates TO. An allosteric model for control of pore opening by substrate binding in the EutL microcompartment shell protein. Protein Sci. 2015;24:956–75. [PubMed: 25752492]

[165]. Sutter M, Greber B, Aussignargues C, Kerfeld CA. Assembly principles and structure of a 6.5-MDa bacterial microcompartment shell. Science. 2017;356:1293–7. [PubMed: 28642439]

[166]. Greber BJ, Sutter M, Kerfeld CA. The plasticity of molecular interactions governs bacterial microcompartment shell assembly. Structure. 2019;27:749–63.e4. [PubMed: 30833088]

[167]. Sutter M, Laughlin TG, Sloan NB, Serwas D, Davies KM, Kerfeld CA. Structure of a synthetic β-carboxysome shell. Plant Physiol. 2019;181:1050–8. [PubMed: 31501298]

[168]. Garcia-Alles LF, Lesniewska E, Root K, Aubry N, Pocholle N, Mendoza CI, Bourillot E, Barylyuk K, Pompon D, Zenobi R, Reguera D, Truan G. Spontaneous non-canonical assembly of CcmK hexameric components from β-carboxysome shells of cyanobacteria. PLoS ONE. 2017;12:1–30.

[169]. Yeates TO, Crowley CS, Tanaka S. Bacterial microcompartment organelles: Protein shell structure and evolution. Ann Rev Biophys. 2010;39:185–205. [PubMed: 20192762]

[170]. Kerfeld CA, Sawaya MR, Tanaka S, Nguyen CV, Phillips M, Beeby M, Yeates TO. Microbiology: Protein structures forming the shell of primitive bacterial organelles. Science. 2005;309:936–8. [PubMed: 16081736]

[171]. Pang A, Frank S, Brown I, Warren MJ, Pickersgill RW. Structural insights into higher order assembly and function of the bacterial microcompartment protein PduA. J Biol Chem. 2014;289:22377–84. [PubMed: 24873823]

[172]. Sutter M, Faulkner M, Aussignargues C, Paasch BC, Barrett S, Kerfeld CA, Liu LN. Visualization of bacterial microcompartment facet assembly using high-speed atomic force microscopy. Nano Lett. 2016;16:1590–5. [PubMed: 26617073]

[173]. Faulkner M, Zhao LS, Barrett S, Liu LN. Self-assembly, stability, and variability of bacterial microcompartment shell proteins in response to environmental change. Nano Res Let. 2019;14:0–7.

[174]. Park J, Chun S, Bobik TA, Houk KN, Yeates TO. Molecular dynamics simulations of selective metabolite transport across the propanediol bacterial microcompartment shell. J Phys Chem B. 2017;121:8149–54. [PubMed: 28829618]

[175]. Lehman BP, Chowdhury C, Bobik TA. The N-terminus of the PduB protein binds the protein shell of the Pdu microcompartment to its enzymatic core. J Bacteriol. 2017;199:1–13.

[176]. Cai F, Sutter M, Cameron JC, Stanley DN, Kinney JN, Kerfeld CA. The structure of CcmP, a tandem bacterial microcompartment domain protein from the β-carboxysome, forms a subcompartment within a microcompartment. J Biol Chem. 2013;288:16055–63. [PubMed: 23572529]

[177]. Larsson AM, Hasse D, Valegård K, Andersson I. Crystal structures of β-carboxysome shell protein CcmP: ligand binding correlates with the closed or open central pore. J Exp Bot. 2017;68:3857–67. [PubMed: 28369612]

[178]. Klein MG, Zwart P, Bagby SC, Cai F, Chisholm SW, Heinhorst S, Cannon GC, Kerfeld CA. Identification and structural analysis of a novel carboxysome shell protein with implications for metabolite transport. J Mol Biol. 2009;392:319–33. [PubMed: 19328811]

[179]. Chowdhury C, Bobik TA. Engineering the PduT shell protein to modify the permeability of the 1,2-propanediol microcompartment of Salmonella. Microbio. 2019;165:1355–64.

[180]. Cannon GC, Shively JM. Characterization of a homogenous preparation of carboxysomes from Thiobacillus neapolitanus. Arch Microbiol. 1983;134:52–9.

[181]. Lassila JK, Bernstein SL, Kinney JN, Axen SD, Kerfeld CA. Assembly of robust bacterial microcompartment shells using building blocks from an organelle of unknown function. J Mol Biol. 2014;426:2217–28. [PubMed: 24631000]

[182]. Mohajerani F, Hagan MF. The role of the encapsulated cargo in microcompartment assembly. PLoS Comp Biol. 2018;14:1–25.

[183]. Rotskoff GM, Geissler PL. Robust nonequilibrium pathways to microcompartment assembly. Proc Natl Acad Sci. 2018;115:6341–6. [PubMed: 29866851]

[184]. Kerfeld CA, Melnicki MR. Assembly, function and evolution of cyanobacterial carboxysomes. Curr Opin Plant Biol. 2016;31:66–75. [PubMed: 27060669]

[185]. Dai W, Chen M, Myers C, Ludtke SJ, Pettitt BM, King JA, Schmid MF, Chiu W. Visualizing individual RuBisCO and its assembly into carboxysomes in marine cyanobacteria by cryo-electron tomography. J Mol Biol. 2018;430:4156–67. [PubMed: 30138616]

[186]. Hagen A, Sutter M, Sloan N, Kerfeld CA. Programmed loading and rapid purification of engineered bacterial microcompartment shells. Nature Coms. 2018;9:1–10.

[187]. Jorda J, Liu Y, Bobik TA, Yeates TO. Exploring bacterial organelle interactomes: A model of the protein-protein interaction network in the Pdu microcompartment. PLoS Comp Biol. 2015;11:e1004067.

[188]. Kennedy NW, Hershewe JM, Nichols TM, Roth EW, Wilke CD, Mills CE, Jewett MC, Tullman-Ercek D. Apparent size and morphology of bacterial microcompartments varies with technique. PLoS ONE. 2020;15:e0226395. [PubMed: 32150579]

[189]. Parsons JB, Dinesh SD, Deery E, Leech HK, Brindley AA, Heldt D, Frank S, Smales CM, Lünsdorf H, Rambach A, Gass MH, Bleloch A, Mcclean KJ, Munro AW, Rigby SEJ, Warren MJ, Prentice MB. Biochemical and structural insights into bacterial organelle form and biogenesis. J Biol Chem. 2008;283:14366–75. [PubMed: 18332146]

[190]. Graf L, Wu K, Wilson JW. Transfer and analysis of Salmonella pdu genes in a range of gram-negative bacteria demonstrate exogenous microcompartment expression across a variety of species. Microb Biotechnol. 2018;11:199–210. [PubMed: 28967207]

[191]. Fang Y, Huang F, Faulkner M, Jiang Q, Dykes GF, Yang M, Liu LN. Engineering and modulating functional cyanobacterial CO2-fixing organelles. Front Plant Sci. 2018;9:1–12. [PubMed: 29410674]

[192]. Bonacci W, Teng PK, Afonso B, Niederholtmeyer H, Grob P, Silver PA, Savage DF. Modularity of a carbon-fixing protein organelle. Proc Natl Acad Sci. 2012;109:478–83. [PubMed: 22184212]

[193]. Long BM, Hee WY, Sharwood RE, Rae BD, Kaines S, Lim YL, Nguyen ND, Massey B, Bala S, Von Caemmerer S, Badger MR, Price GD. Carboxysome encapsulation of the CO2-fixing enzyme Rubisco in tobacco chloroplasts. Nature Coms. 2018;9.

[194]. Lee MJ, Palmer DJ, Warren MJ. Biotechnological advances in bacterial microcompartment technology. Trends Biotechnol. 2019;37:325–36. [PubMed: 30236905]

[195]. Young EJ, Burton R, Mahalik JP, Sumpter BG, Fuentes-Cabrera M, Kerfeld CA, Ducat DC. Engineering the bacterial microcompartment domain for molecular scaffolding applications. Front Microbiol. 2017;8:1–9. [PubMed: 28197127]

[196]. Chessher A, Breitling R, Takano E. Bacterial microcompartments: Biomaterials for synthetic biology-based compartmentalization strategies. ACS Biomat Sci Engr. 2015;1:345–51.

[197]. Corchero JL, Cedano J. Self-assembling, protein-based intracellular bacterial organelles: Emerging vehicles for encapsulating, targeting and delivering therapeutical cargoes. Microb Cell Fact. 2011;10:1–8. [PubMed: 21211066]

[198]. Planamente S, Frank S. Bio-engineering of bacterial microcompartments: A mini review. Biochem Soc Trans. 2019;47:765–77. [PubMed: 31235547]

[199]. Bari NK, Kumar G, Hazra JP, Kaur S, Sinha S. Functional protein shells fabricated from the self-assembling protein sheets of prokaryotic organelles. J Mater Chem B. 2020;8:523–33. [PubMed: 31845931]

[200]. Jorda J, Leibly DJ, Thompson MC, Yeates TO. Structure of a novel 13-nm dodecahedral nanocage assembled from a redesigned bacterial microcompartment shell protein. Chem Commun. 2016;52:5041–4.

[201]. Sutter M, Mcguire S, Ferlez B, Kerfeld CA. Structural characterization of a synthetic tandem-domain bacterial microcompartment shell protein capable of forming icosahedral shell assemblies. ACS Synth Bio. 2019;8:668–74. [PubMed: 30901520]

[202]. Ferlez B, Sutter M, Kerfeld CA. A designed bacterial microcompartment shell with tunable composition and precision cargo loading. Metab Eng. 2019;54:286–91. [PubMed: 31075444]

[203]. Liang M, Frank S, Lünsdorf H, Warren MJ, Prentice MB. Bacterial microcompartment-directed polyphosphate kinase promotes stable polyphosphate accumulation in E. coli. Biotechnol J. 2017;12.

[204]. Huber I, Palmer DJ, Ludwig KN, Brown IR, Warren MJ, Frunzke J. Construction of recombinant Pdu metabolosome shells for small molecule production in Corynebacterium glutamicum. ACS Synth Bio. 2017;6:2145–56. [PubMed: 28826205]

[205]. Nichols TM, Kennedy NW, Tullman-Ercek D. Cargo encapsulation in bacterial microcompartments: methods and analysis. Methods Enzymol. 2019;617:155–86. [PubMed: 30784401]

[206]. Wade Y, Daniel RA, Leak DJ. Heterologous microcompartment assembly in bacillaceae: Establishing the components necessary for scaffold formation. ACS Synth Bio. 2019;8:1642–54. [PubMed: 31242391]

[207]. Yung MC, Bourguet FA, Carpenter TS, Coleman MA. Re-directing bacterial microcompartment systems to enhance recombinant expression of lysis Protein E from bacteriophage φX174 in Escherichia coli. Microb Cell Fact. 2017;16:1–17. [PubMed: 28049473]

[208]. Lee MJ, Mantell J, Brown IR, Fletcher JM, Verkade P, Pickersgill RW, Woolfson DN, Frank S, Warren MJ. De novo targeting to the cytoplasmic and luminal side of bacterial microcompartments. Nature Coms. 2018;9:1–11.

[209]. Bari NK, Kumar G, Bhatt A, Hazra JP, Garg A, Ali ME, Sinha S. Nanoparticle fabrication on bacterial microcompartment surface for the development of hybrid enzyme-inorganic catalyst. ACS Catal. 2018;8:7742–8.

[210]. Cameron JC, Wilson SC, Bernstein SL, Kerfeld CA. Biogenesis of a bacterial organelle: The carboxysome assembly pathway. Cell. 2013;155:1131. [PubMed: 24267892]

[211]. Iancu CV, Morris DM, Dou Z, Heinhorst S, Cannon GC, Jensen GJ. Organization, structure, and assembly of α-carboxysomes determined by electron cryotomography of intact cells. J Mol Biol. 2010;396:105–17. [PubMed: 19925807]
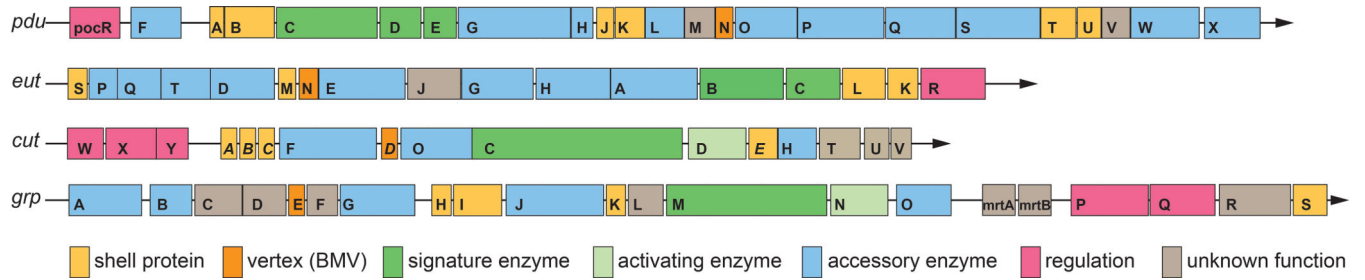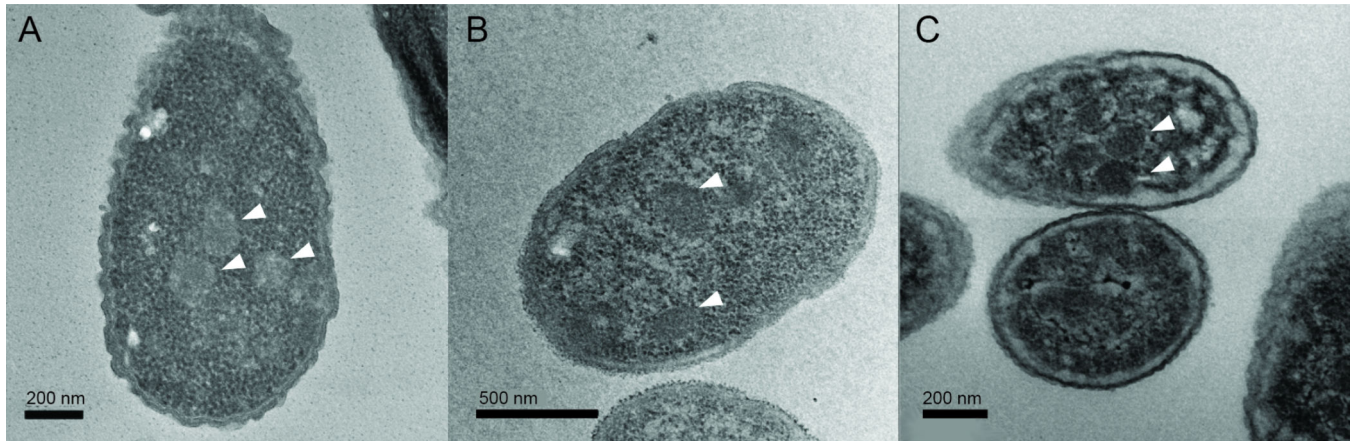
Figure 1:
A comparison of selected MCP operons. Representative operons from *S. enterica* LT2 (*pdu*, *eut*), *E. coli* 536 (*cut*), and *E. coli* CFT073 (*grp*) are shown using one-letter abbreviations for genes and protein products. Gene sizes and spacing are roughly to scale.

*Note that in the *cut* operon, shell proteins are named with a different acronym, *CmcA-E* to avoid redundancy with prior work.
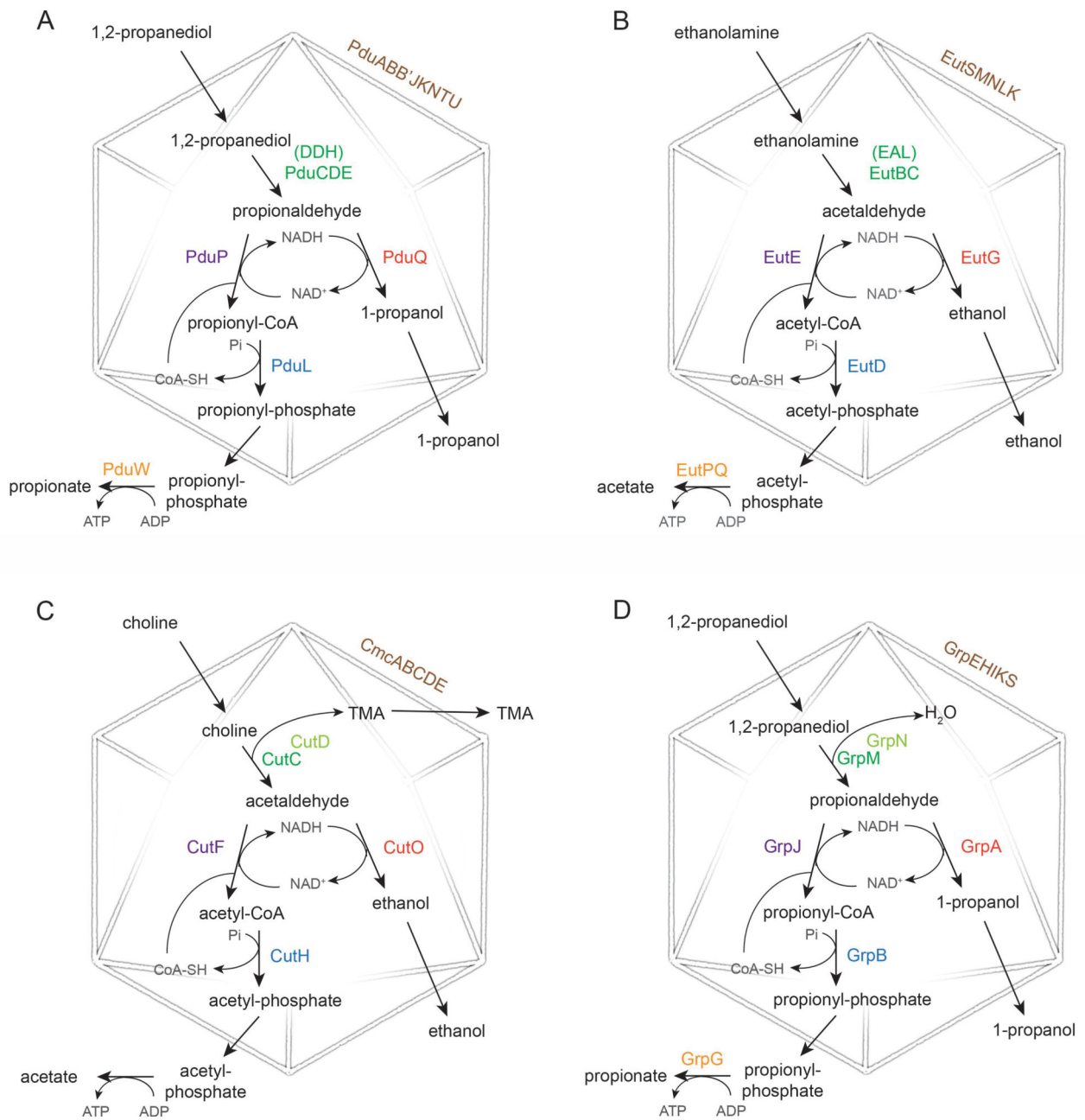
Figure 2:
Schematic of MCP pathways discussed in the text. A) Pdu MCP B) Eut MCP C) Cut MCP
D) Grp MCP. Shell proteins names are shown in brown, signature enzymes in green,
accessory enzymes (where applicable) in light green, aldehyde dehydrogenase in purple,
alcohol dehydrogenase in red, phosphotransacetylase in blue, and acetate kinase in gold.

Figure 3:
Electron micrographs of bacteria expressing MCPs, indicated by arrows: A) Cut MCPs from *E. coli* 536; B) Grp MCPs from *E. Coli* CFT073; C) Pdu MCPs from *S. enterica*. Scale bars are located on each image. Images were obtained as described [76].
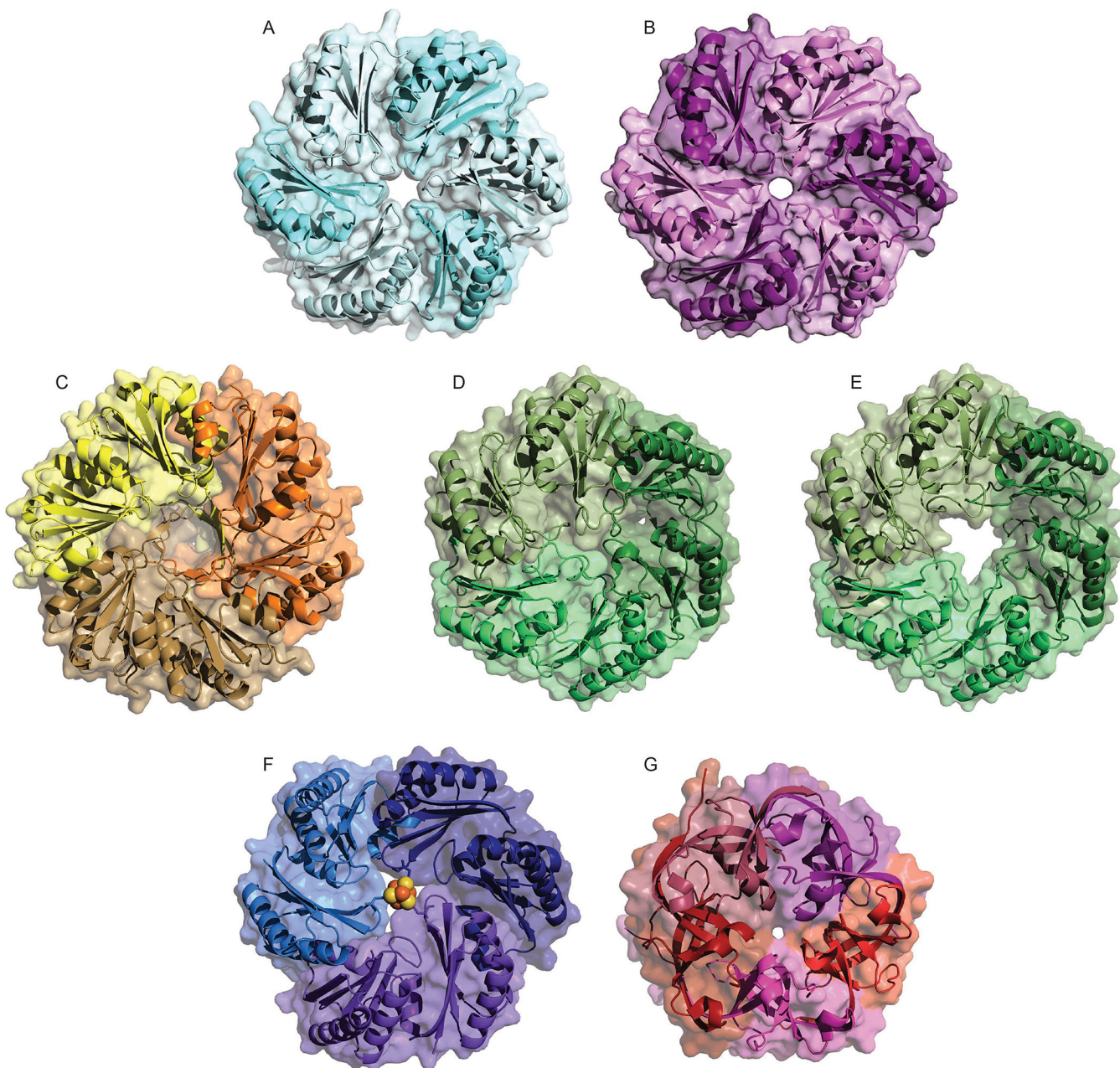
Figure 4:

Representative crystal structures of select MCP shell proteins. A) PduA BMC-H protein from *S. enterica typhimurium* (PDB ID: 3NGK) [155], B) EutM, the orthologous BMC-H protein from *E. coli* K-12 (3I6P) [159] C) PduU permuted BMC-H protein from *S. enterica typhimurium* (3CGI) [154], D) EutL BMC-T closed form from *E. coli* K12 (3GFH) [160], E) EutL BMC-T open form from *E. coli* K12 (3I87) [159], F) PduT [Fe-S]-containing BMC-T protein from *C. freundii* (3PAC) [156], G) GrpN BMV pentamer from *R. rubrum* (4I7A) [158]

Table 1:

MCP operons found in *S. enterica* and *E. coli*, taken from genomic studies [4]. See reference methodology for details. Multiple strains of the same Serovar are listed in the first instance.

Salmonella enterica

NCBI Taxon ID	serovar	strain	MCP locus	
41514	Arizonae	62:z4,z23:-	PDU	EUT
882884		62:z4,z23:- RSK2980	PDU	EUT
454166	Agona	SL483	PDU	EUT
321314	Choleraesuis	SC-B67	PDU	EUT
439851	Dublin	CT_02021853	PDU	EUT
550537	Enteritidis	P125109	PDU	EUT
550538	Gallinarum	287/91	PDU	EUT
1081093	Gallinarum/pullorum	-	PDU	EUT
454169	Heidelberg	SL476	PDU	EUT
1267753	Javiana	CFSAN001992	PDU	EUT
423368	Newport	SL254	PDU	EUT
295319	Paratyphi A	ATCC 9150	PDU	EUT
1016998	Paratyphi B	SPB7	PDU	EUT
476213	Paratyphi C	RKS4594	PDU	EUT
439843	Schwarzengrund	CVM19633	PDU	EUT
220341	Typhi	CT18	PDU	EUT
1132507		P-stx-12	PDU	EUT
209261		Ty2	PDU	EUT
527001		Ty21a	PDU	EUT
588858	Typhimurium	14028S	PDU	EUT
568708		D23580	PDU	EUT
99278		LT2	PDU	EUT
216597		SL1344	PDU	EUT
990282		UK-1	PDU	EUT
936157	Weltevreden	2007-60-3289-1	PDU	EUT

Escherichia coli

NCBI Taxon ID	serovar	strain	MCP Locus		
216592	042	-		EUT	
362663	536	-		EUT	CUT
655817	ABU 83972	-		EUT	
405955	APEC O1	-		EUT	GRP
469008	BL21(DE3)	-		EUT	
199310	CFT073	-		EUT	GRP
331111	E24377A	-	PDU	EUT	
585397	ED1a	-		EUT	GRP

585057	IAI39	-		EUT	CUT
595495	KO11FL	-		EUT	
591946	LF82	-	PDU	EUT	
574521	O127:H6	E2348/69	PDU	EUT	
155864	O157:H7	EDL933		EUT	
386585	O157:H7	Sakai		EUT	
1072459	O7:K1	CE10		EUT	CUT
585035	S88	-		EUT	GRP
409438	SE11	-		EUT	
439855	SMS-3-5	-		EUT	
511145	K-12	MG1655		EUT	
585056	UMN026	-	PDU	EUT	
696406	UMNK88	-		EUT	
364106	UTI89	-		EUT	CUT